



Controls of the partitioning of nitrate between DNRA and denitrifiers

Frida Lindvall

Degree project/Independent project • 30 credits
Swedish University of Agricultural Sciences, SLU
Department of Forest Mycology and Plant Pathology
Agriculture Programme – Soil and Plant Sciences
Uppsala 2022



Controls of the partitioning of nitrate between DNRA and denitrifiers

Frida Lindvall

Supervisor: Aurélien Saghai, SLU, Forest Mycology and Plant Pathology
Examiner: Hanna Friberg, SLU, Forest Mycology and Plant Pathology

Credits: 30 credits
Level: A2E
Course title: Master thesis in Biology
Course code: EX0898
Programme: Agriculture Programme - Soil/Plant
Course coordinating dept: Department of Aquatic Sciences and Assessment
Place of publication: Uppsala
Year of publication: 2022
Copyright: All featured images are used with permission from the copyright owner.

Keywords: DNRA, denitrification, microcosm experiment, arable soil

Swedish University of Agricultural Sciences

The Faculty of Natural Resources and Agricultural Sciences
Department of Forest Mycology and Plant Pathology
Soil microbiology

Abstract

In arable soils, the importance of denitrification, a respiratory process where nitrate (NO_3^-) is stepwisely reduced to nitrogen gas and nitrous oxide (N_2O) is well established. More recently has dissimilatory nitrate reduction to ammonium (DNRA) gained interest as its importance in agricultural soils might have been largely overlooked. Since these two functional microbial groups both utilize NO_3^- as an electron acceptor for anaerobic respiration they are competing in the soil. One pathway can produce a potent greenhouse gas (N_2O) while the other is producing plant available nitrogen, for this reason it is of importance to try to understand what factors can promote DNRA over denitrification

This experiment aims to study what drivers control the partitioning of NO_3^- between denitrifiers and DNRA in an agricultural soil. It also serves as a pilot for a bigger study aimed to compare the effect of these drivers on soil with different management history. Soil was incubated under anoxic conditions and resources in form of organic carbon (C) and NO_3^- were added in different ratios (C: NO_3^- ratios) and amounts. We hypothesised that there would be differences related to the either C: NO_3^- ratio and/or amounts and that low ratios and/or high NO_3^- amounts will promote denitrification whereas high NO_3^- ratios and/or NO_3^- nitrogen amounts will promote DNRA.

The microcosms were destructively sampled at seven different timepoints. Gas samples from the headspace in the microcosms were analysed by gas chromatography for N_2O . Soil samples were used for soil nitrogen and DNA extractions. Quantitative real-time PCR was performed on the denitrification marker gene *nir*, the DNRA marker gene *nrfA* and the 16S rRNA gene for assessing overall bacterial and archaeal community size. This experiment showed that DNRA was more abundant than denitrifiers, whereas most studies show the opposite. Further, the genetic potential for DNRA was continually high across the treatments. It was only somewhat lower for a treatment with a C: NO_3^- ratio of 4, with C amount equivalent to 8000 kg/ha and NO_3^- amount equal to 200 kg/ha, also for which genetic potential for denitrification was the highest. This experiment suggests that not C: NO_3^- ratio but a high amount of NO_3^- and carbon promotes denitrification on the expense of the otherwise continually high DNRA in the studied soil.

Keywords: DNRA, denitrification, microcosm experiment, arable soil

Table of contents

List of tables	6
List of figures.....	7
Abbreviations	8
1. Introduction	9
1.1 Background.....	9
1.2 Denitrification	10
1.3 Dissimilatory nitrate reduction to ammonium	12
1.4 Environmental factors affecting the competition for NO ₃ ⁻	12
1.5 Aim and objectives	14
2. Materials and Methods	16
2.1 The soil.....	16
2.2 The microcosms – experiment set up	17
2.3 Assessing microbial functional guilds	18
2.3.1 DNA extraction.....	18
2.3.2 Quantitative PCR of marker genes	19
2.1 Ammonium and nitrate measurements in soil samples	22
2.1.1 Ammonium- and nitrate-nitrogen extraction	22
2.1.2 Analysis with SEAL AutoAnalyzer 500	23
2.1 Nitrous oxide measurements	23
2.1.1 Gas chromatography	23
2.2 Data analysis.....	25
3. Results	26
3.1 Soil nitrogen content	26
3.2 Nitrous oxide	30
3.3 Microbial functional guilds	32
3.3.1 Bacterial and archaeal abundance	32
3.3.2 Abundance of denitrifiers	34
3.3.3 Abundance of DNRA	38
3.4 Correlation study	42
4. Discussion	48
4.1 Effect of C:NO ₃ ⁻ ratio and amount nitrate respiration pathway over time	48
4.2 Correlations between changes in N pools and/or net N ₂ O production and the abundance of functional communities	52
4.3 Take-aways from this pilot study and method discussion	53
5. Conclusions.....	56
References	57
Popular science summary.....	60
Acknowledgements.....	61
Appendix 1	62

List of tables

Table 1: Experiment set up with fertilisation treatments, carbon and nitrate equivalents in kilogram per hectare and the carbon:nitrate ratios.	18
Table 2: Inhibition test with M13 plasmid for qPCR quantification with primers, master mix composition in concentrations per reaction and protocol	20
Table 3: qPCR quantification of 16S rRNA marker gene with primers, master mix recipe in concentrations per reaction and protocol.....	20
Table 4: qPCR quantification of <i>nirK</i> marker gene with primers, master mix composition in concentrations per reaction and protocol.....	21
Table 5: qPCR quantification of <i>nirS</i> marker gene with primers, master mix composition in concentrations per reaction and protocol.....	21
Table 6: qPCR quantification of <i>nrfA</i> marker gene with primers, master mix composition in concentrations per reaction and protocol.....	22
Table 7: Statistical analysis of differences in nitrate concentration across the different treatments.	28
Table 8: Statistical analysis of differences in ammonium concentration across treatments	30
Table 9: Statistical analysis of differences in net nitrous oxide production across the different treatments	32
Table 10: Statistical analysis of differences in absolute abundance of the prokaryotic marker gene 16S rRNA across the different treatments.....	34
Table 11: Statistical analysis of differences in absolute abundance of the <i>nir</i> marker gene across the different treatments.	36
Table 12: Statistical analysis of differences in relative abundance of the <i>nir</i> marker gene across the different treatments.	38
Table 13: Statistical analysis of differences in absolute abundance of the <i>nrfA</i> marker gene across the different treatments.	39
Table 14: Statistical analysis of differences in relative abundance of the <i>nrfA</i> marker gene across the different treatments.	41
Table 15: Statistical analysis of differences in relative abundance of <i>nrfA/nir</i> ratio across the different treatments	42
Table 16: Correlations between variables tested with the Spearman's correlation test. .	43

List of figures

Figure 1: The microbial pathways of the nitrogen cycle (Hallin et al. 2018).....	10
Figure 2: Illustration of the microcosm set up.	17
Figure 3: Gas sampling of microcosm headspaces and standard curves for calculating N ₂ O concentration.....	24
Figure 4: Nitrate concentrations in soil extracts	27
Figure 5: Ammonium concentration in soil extracts	29
Figure 6: Nitrous oxide concentration from gas headspaces	31
Figure 7: Absolute abundance of the prokaryotic marker gene 16S rRNA.	33
Figure 8: Absolute abundance of the functional marker genes nirK and nirS.....	35
Figure 9: Relative abundance of the functional genes nirK and nirS	37
Figure 10: Absolute abundance of the functional marker gene nrfA.....	39
Figure 11: Relative abundance of the functional gene nrfA.	40
Figure 12: Functional gene nrfA/functional nirK and nirS.....	41
Figure 13: NO ₃ ⁻ concentration in the incubated soil compared to N ₂ O concentration	44
Figure 14: NH ₄ ⁺ concentration in the incubated soil compared to the relative abundances of the nrfA marker gene	45
Figure 15: Marker gene nir abundance in the incubated soil compared to N ₂ O concentration in the headspaces	45
Figure 16: Marker gene nrfA abundance in the incubated soil compared to N ₂ O concentration in the headspaces	46
Figure 17: The ratio between marker gene nrfA/nir in the incubated soil compared to N ₂ O concentration in the headspaces	47

Abbreviations

DNRA	Dissimilatory nitrate reduction to ammonium
GHG	Greenhouse gas
WHC	Water holding capacity

1. Introduction

1.1 Background

A growing human population demands an increased food production, besides a need for increased efficiency in the distribution of food products. Nitrogen has been identified as one of the main limitations for plant production (Schlesinger & Bernhardt 2013). It has also been pointed out as a resource that we currently use to an extent that exceeds the planetary boundaries (Steffen et al. 2015). Nitrogen fertilisation can be applied in different organic forms to be mineralised in the soil, or in different mineral forms, as ammonium (NH_4^+) and nitrate (NO_3^-). Along with the challenge to increase production there are urgent environmental and ecological problems such as greenhouse gas (GHG) emissions and NO_3^- leaching. Hence, the agricultural sector is challenged to increase production while mitigating climate change and pollution.

In this context, NO_3^- is an important molecule. It can be assimilated by plants although it has been suggested that NH_4^+ is the preferred nitrogen source since it can enter the amino acid production directly while NO_3^- must be transformed to ammonium before it can be utilized (Hachiya & Sakakibara 2017). Later observations do, however, suggest that a mixture of both forms is most efficient for plant growth. Nitrate is often used in mineral fertilisers where it has the advantage, compared to NH_4^+ , that it is less volatile (Dari et al. 2019). The disadvantage, on the other hand, is that it does not bind as well to soil particles due its negative charge and therefore can leak from the field and cause eutrophication in nearby waterbodies (Oelmann et al. 2007). Nitrate is also a desirable electron acceptor for respiration in anoxic environments (Hayatsu et al. 2008). One possible outcome of this reduction is the formation and emission of nitrous oxide (N_2O). N_2O is a GHG with a potency 300 times that of carbon dioxide on a 100-year time scale (IPCC 2007). Fertilisation with mineral fertilizers has been shown to be one of the most important sources of N_2O production and emissions (Lebender et al. 2014). It has also been shown to be the most important molecule for ozone depletion today and is predicted to continue to be so throughout this century (Ravishankara et al. 2009).

The two main anoxic respiratory strategies for utilizing nitrate are the denitrification process and dissimilatory nitrate reduction to ammonium (DNRA). They, together with the other major nitrogen transformation processes, are visualized in figure 1 by Hallin et al. (2018).

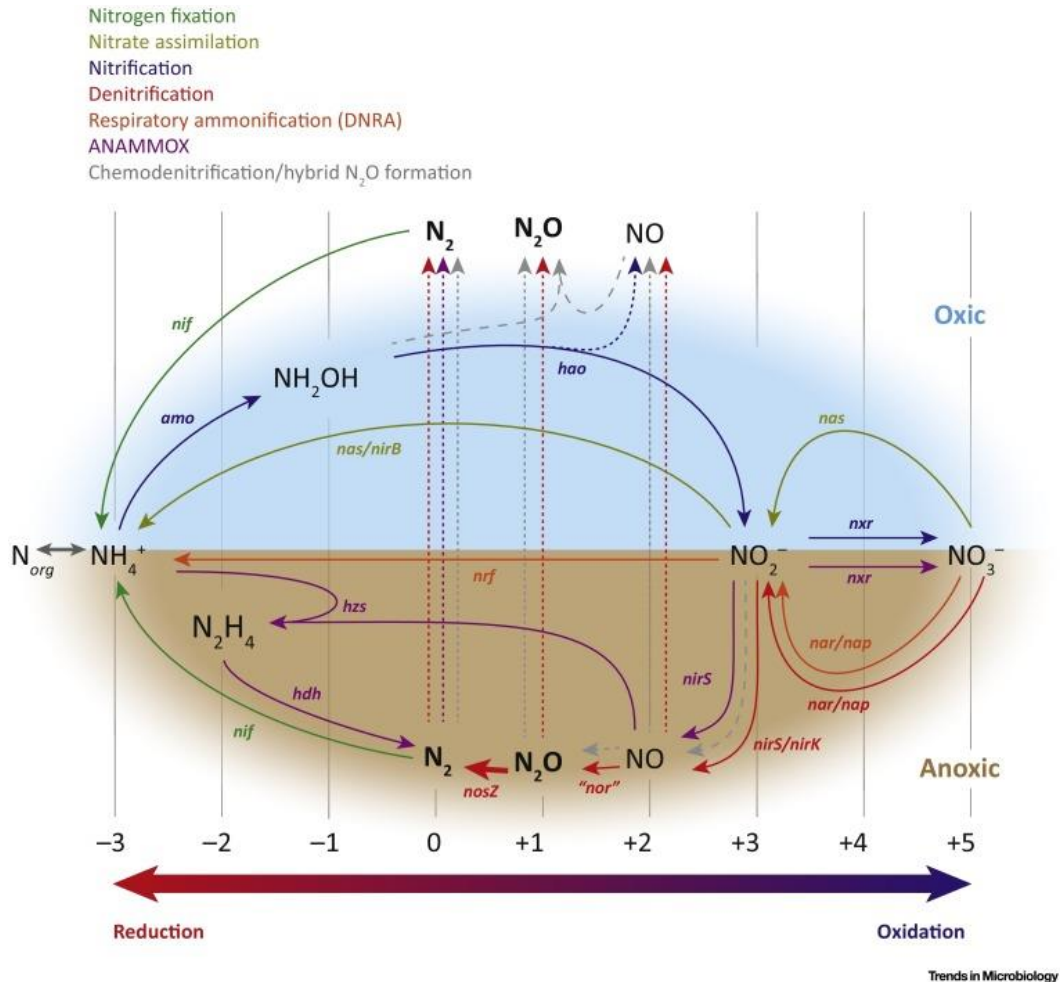


Figure 1: The microbial pathways of the nitrogen cycle (Hallin et al. 2018). The compounds are arranged in order of oxidation state (left is more reduced while right is more oxidised), the orange and blue colours indicate whether the reaction occurs under oxic or anoxic conditions. Solid lines indicate microbial pathways and the names of the genes that encode the enzymes catalysing the reactions are indicated. Denitrification is indicated with red coloured arrows, dissimilatory nitrate reduction to ammonia (DNRA) in orange and nitrification in blue.

1.2 Denitrification

Denitrification is a modular process where NO₃⁻ is reduced to N₂ in several steps (Fig. 1). It is a form of anaerobic respiration that is facultative within many microorganisms. NO₃⁻ is reduced in four steps catalysed by four distinct enzymes. First, NO₃⁻ is reduced to nitrite (NO₂⁻) by either the periplasmic Nap nitrate

reductase complex encoded by the *napAB* gene cluster or the membrane-bound Nar nitrate reductase complex present in bacteria, encoded by the *narGH* gene cluster (Kraft et al. 2011). NO_2^- is then reduced to nitric oxide (NO) by the periplasmic nitrite reductase enzymes NirK and NirS, encoded by the similarly named *nirK* and *nirS* genes. They are evolutionary unrelated but are deemed to have the same function. NO is then reduced to nitrous oxide (N_2O) by nitric oxide reductase enzymes Nor. NO_2^- and NO are free radicals that can cause harm to the cell, which is why accumulation must be prevented. There are a couple of different types of Nor enzymes, some that utilizes NO for respiration while the function of others is simply to detoxify NO. Many studies show a co-regulation of Nor and Nir enzymes so that NO is not produced faster than it can be consumed (Körner et al. 2003; Spiro 2007). N_2O is lastly reduced to nitrogen gas (N_2) by the nitrous oxide reductase NosZ, encoded by the *nosZ* gene (Kraft et al. 2011). Complete denitrification with N_2 as the end-product is not directly environmentally harmful but a path for once fixed nitrogen to return to the atmosphere. In the agricultural context it is, however, a loss of valuable soil nitrogen. Most importantly, denitrification is a modular process and is, more than often, not complete, since only about 40% of denitrifiers carries the *nosZ* gene to reduce N_2O to N_2 (Graf et al. 2014). This is one of the main sources of N_2O emissions from agricultural soil.

Denitrification is often called an anaerobic process since transcriptional regulators are sensitive to oxygen (O_2) and will inhibit NO_3^- uptake by the cell under oxic conditions (Moir & Wood 2001; Körner et al. 2003). There are, however, cases where denitrifying organism with periplasmic nitrate reductase reduces NO_3^- under oxic condition since no transport of NO_3^- to the cytoplasm is needed, Trevors (1985) has found occurrences of aerobic denitrification in soil. Respiration with O_2 would however be more advantageous for organisms with that ability (Prescott et al. 1996). Furthermore, the last step of denitrification, N_2O reduction, is inhibited by O_2 because the enzyme itself is sensitive to it (Frette et al. 1997). This implies that in cases where denitrification takes place in the presence of O_2 there might be an increase of N_2O production.

Denitrification is coupled with the nitrogen transformation process nitrification, where ammonia is oxidised to nitrate (Fig. 1). This occurs under oxic conditions and is, together with NO_3^- fertilisation, the main source of NO_3^- in the soil. Another relevant type of nitrogen transformation is nitrogen mineralisation (Fig. 1). When microorganisms have a shortage of carbon compared to nitrogen, *i.e.* a low C:N ratio, they will free carbon within the cell by removing NH_4^+ from amino acids (Robertson & Groffman 2015). NH_4^+ is released to the environment as a result. The opposite of mineralisation is immobilisation, where NH_4^+ is assimilated for growth when carbon is unlimiting.

1.3 Dissimilatory nitrate reduction to ammonium

Dissimilatory nitrate reduction to ammonium, DNRA, is an anaerobic respiratory pathway where NO_3^- is first reduced to NO_2^- , as in the denitrification process, by the periplasmic Nap nitrate reductase complex or the membrane-bound Nar complex (Kraft et al. 2011). The NO_2^- is then reduced to the end-product, ammonium (NH_4^+), by cytochrome c_{552} or NADH-dependent nitrite reductases NrfA and NirB, respectively (Heo et al. 2020). They are encoded by the genes *nrfA* and *nirB*. NrfA is membrane-bound and resulting in the release of NH_4^+ to the environment while NirB is cytoplasmic, resulting in assimilation of NH_4^+ , hence the terms dissimilatory vs. assimilatory nitrate reduction to ammonium.

DNRA has, in contrary to denitrification, been assumed to not release intermediate products such as NO and N_2O (Einsle et al. 2002). A study by Stremińska et al. (2012) has since given some nuance to this assumption showing N_2O production by DNRA bacteria isolated from soil. They reported 2.7 and 5% nitrate reduction to N_2O with low C: NO_3^- ratio, 5 and 10, and 0.1% and 0.7% with high ratios, 25 and 50. This production is however deemed small in contribution of the total N_2O budget (Rütting et al. 2011; Stremińska et al. 2012). They further state that the C: NO_3^- ratio is relevant for the question of N_2O production by DNRA bacteria.

1.4 Environmental factors affecting the competition for NO_3^-

Both of these NO_3^- -respiration pathways are widespread among different taxonomic groups (Graf et al. 2014; Welsh et al. 2014). One of these respiratory pathways causes N_2O emissions while the other reduce NO_3^- to NH_4^+ , which can then be assimilated by growing crops, as NH_4^+ or, after oxidation, NO_3^- . Hence, with regards to mitigating climate change by lowering greenhouse gas emission and managing resources in sustainable way, it is urgent to develop an understanding for how agricultural management could push the microbiome towards DNRA rather than denitrification.

The ratio between electron acceptor, NO_3^- , and the electron donor, the carbon substrate, is one factor that has received a lot of attention in many recent studies (Yoon et al. 2015; Vuono et al. 2019; Heo et al. 2020; Nojiri et al. 2020). Based on the work by Tiedje et al. (1983) it has been suggested that low C: NO_3^- ratios promote denitrification while high ratios promote DNRA. This is partly explained by Strohm et al. (2007) that calculated that DNRA gains more energy per oxidised

glucose molecule and therefore needs to reduce less NO_3^- for the same amount of energy. It is however probably not as clear-cut since both respiratory pathways are, as mentioned by Graf et al. 2014 and Welsh et al. 2014, taxonomically widespread implying that the metabolism possibly can be widely different from organism to organism. A study by Vuono et al. (2019) challenges this assumption. They used the dual pathway DNRA/denitrification gram-positive Actinobacterium species strain *Intasporangium calvum* C5 to study how different ratios and C and NO_3^- concentration. They found that *I. calvum* C5 use the DNRA pathway when C concentration is low, independent of C: NO_3^- ratio, further suggesting that this trend is due to a lowered intercellular redox potential caused by low carbon resources that lowers the catalytic activity in the electron transport chain that is needed for denitrification enzymes. A recent study by Heo et al. (2020) addresses that soil organisms utilising the DNRA pathway has long been neglected due to lacking isolation and enrichment methods. Using a new colorimetric screening method, they isolated five strains of Proteobacteria covering five different genus and one strain of *Bacillus* sp. within the Firmicutes phylum from rice paddy soils. All isolates had the *nrfA* and or the *nirB* gene, with the *Bacillus* isolate also carrying a *nosZ* gene. They also showed inhibited reduction from NO_2^- to NH_4^+ when NO_3^- concentrations were below 1 mM/L and down regulation of *nrfA* and *nirB* as NO_3^- was reduced. Further, conditions with unlimited electron donors gave NH_4^+ production from NO_3^- reduction while low carbon and unlimited NO_3^- resulted in NO_3^- reduction and NO_2^- accumulation but low NH_4^+ production. This finding is similar to the early observation by Tiedje et al. (1983) but underlines that the observed patterns may be correlated to concentration rather than ratio and that this is due to NO_2^- accumulation but low NH_4^+ production when access to electron acceptors is low.

DNRA vs. denitrification has been studied in dual-pathway organisms isolated from a groundwater well and in isolates from rice paddy soils (Vuono et al. 2019; Heo et al. 2020). In one of the few available field studies Putz et al. (2018) studied DNRA and denitrification activity in an agricultural soil. They used functional gene quantification and ^{15}N tracing to compare the impact of two crop rotations, one with cereal and one with cereal and ley. They predicted higher ammonification, higher DNRA activity in the soil with the ley crop rotation since it had higher amounts of soil organic matter (SOM). This was also what they found and stated that management can impact microbiome to conserve soil nitrogen. However, the abundance of each of the denitrification marker genes outnumbered the DNRA marker gene by 5-10 times.

For the assay, they used three types of added ^{15}N labelled nitrogen resources: NO_3^- , NH_4^+ and a combination of both, these created microcosms where destructively

sampled at different timepoints ranging over 24 h in total, for soil nitrogen, NO_3^- , NH_4^+ , and N_2O in the gas headspace. Putz et al. (2018) studied soil from two fertilisation strategies, with no and fertilisation conventional, with treatments equivalent to 120 kg N/ha for the cereal rotation and 150 kg N/ha for the cereal-ley rotation.

While they state, as their nitrogen measurements from the microcosm experiment with labelled nitrogen imply, that management impacts microbiome and its functionality they do not sample and quantify the marker genes over the different timepoints. It is not certain that they would have found any differences over the relatively short 24-hour incubation. However, from this experiment it is unclear how lasting any impact of management is. Would the microbiome change immediately by a treatment different from the long term-management, or in field terms if a different crop and fertilisation strategy was used just for one growth period? Is the effect of management history so short term that it would be more accurately described as an effect of the state the soil was in just at sampling? What are the drivers that change microbiome functionality, pushes it towards either denitrification or DNRA, how long lasting are the effects of one specific treatment?

The type of microcosm experiment Putz et al. (2018) used for tracing nitrogen flow could be used to test for effects over a longer time-period and compare different C: NO_3^- ratio and amounts of added resources to soil under anoxic incubation. Sampling would then include functional genes, soil nitrogen pools and microcosm headspace N_2O at different timepoints.

1.5 Aim and objectives

Through this experiment we aimed to (i) study how the addition of different carbon and nitrate resource ratios affect the competition for NO_3^- between DNRA and denitrifiers over time in a microcosm experiment. Soil N pools, NO_3^- and NH_4^+ , and cumulative N_2O emissions were measured to (ii) clarify if previous findings on the impact of C: NO_3^- ratio and C and NO_3^- hold for the soil used, one collected from an experimental site at Lönnstorp research station, Sweden. The experiment also aimed to (iii) serve as a pilot study for a long-term microcosm experiment. The pilot study would assess the suitable time range between addition of resources (pulses) for studying changes in the genetic potential for NO_3^- respiration in relation to resource availability/consumption over longer periods of time.

More specifically, we aimed to address the following questions:

- How does the genetic potential for NO_3^- respiration, measured as the number

of copies of functional marker genes *nirK*, *nirS* and *nrfA*, change over time with addition of different C and NO₃⁻ ratios and amounts?

- Are there correlations between changes in N pools and/or net N₂O production and the abundance of the functional communities?
- What are the most important take-aways from the experiment for application on a larger experiment comparing different managements, crop rotation and harvest residue management, within the same soil?

Hypothesis:

- Treatments with different C:NO₃⁻ ratios and/or NO₃⁻ amounts affect the measurements differently.
- Low C:NO₃⁻ ratios and/or high NO₃⁻ amounts promote denitrification, hence higher *nir* abundance and net N₂O production (Putz et al. 2018).
- High C:NO₃⁻ ratios and/or low NO₃⁻ amounts promote DNRA, hence higher *nrfA* abundance and abundance and net N₂O production (Putz et al. 2018)

2. Materials and Methods

For the methods the soil was chosen and analysed for soil characteristics, the experiment with microcosms were set up. The microcosms were after incubation sampled for three analyses: gas samples for studying the net N₂O production through gas chromatography, soil samples for quantifying the denitrifiers and DNRA through quantitative real-time PCR and soil samples to analyse inorganic soil nitrogen in the soil through spectrophotometry. Further, the experiment was set-up with five treatments, including different levels of NO₃⁻ and a carbon cocktail. The microcosms were destructively sampled at seven timepoints to study them over time. The following sections explain the choice of soil, its characteristics, the experiment set up and the methods in detail.

2.1 The soil

This experiment was performed with soil from the SLU research station Lönnstorp (located near Alnarp, Sweden), from the long-term experiment R3-0020 studying the humus balance in cereal rotations. The crop rotation is composed solely by cereal crops, including wheat, barley and oat (Bergkvist & Oborn 2011).

The soil for the experiment was collected in October 2020, sieved at 4 mm, and stored at -20 °C. A soil from the one of the R3-0020 treatments, with 40 kg/ha nitrogen fertilisation and ploughed down straw was used in the experiment. This soil was chosen to inform a future and more extensive experiment, comparing the legacy effects of fertilisation strategies and harvest residue management on the partitioning nitrate between denitrifiers and DNRA. It should be noted that the fertilisation strategy of the soil is not representative of common fertilisation practice for cereal production.

Soils from the four replicates were thawed at room temperature and mixed in a plastic tray with a hand shovel sterilised with 70% ethanol into a composite sample. Water content and water holding capacity (WHC) were measured on the composite sample. The clay content was 20% and pH 6.5.

2.2 The microcosms – experiment set up

Portions of 100 g fresh weight soil was placed in 250 ml autoclaved Duran® bottles and 8.6 ml of autoclaved distilled water was added to reach 65% WHC. The soil was mixed by swirling the bottles and flattened out with a spoon to ensure equal conditions in the soil.

The bottles were closed with gas tight caps with rubber stoppers. A gas exchanger was used to replace the air in the bottles by nitrogen gas to create anoxic incubation conditions. The bottles with soil were then incubated in a dark room at 25°C. Release of increasing gas pressure in the bottles was facilitated by water locks made with needles, autoclaved dual caps and tubing that were put into trays with water (Fig. 2).

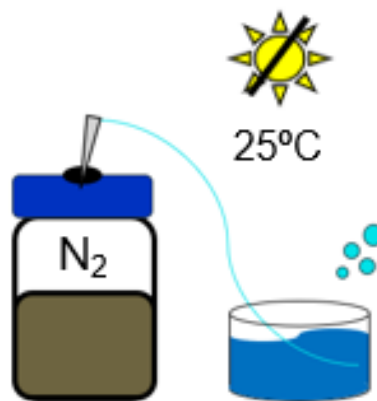


Figure 2: Illustration of the microcosm set up.

The microbial communities were allowed to acclimatise to their new environment for 10 days before the start of the experiment (acclimatisation phase). At this point (T₀), carbon and nitrogen resources were added to the remaining bottles. The carbon cocktail used consisted in equimolar amounts of carbon from acetate, succinate and lactate. This was preferred to a single carbon source since microorganisms are likely to have different preferences for electron donor. The combination of different carbon substrates was thus used to minimise any selective effect (Carlson et al. 2020). Nitrate in the form of potassium nitrate was used as the nitrogen resource. Salts were dissolved in ultrapure water to four different concentrations that, when used to wet the soil in the bottles to 70% WHC, gave it resource concentrations equal to: 8000 kg C and 200 kg NO₃⁻/ha, 8000 kg C and 20 kg NO₃⁻/ha, 800 kg C and 200 kg NO₃⁻/ha, 800 kg C and 20 kg NO₃⁻/ha (Table 1). These treatments were also designed to enable assessments at three different C:NO₃⁻ ratios: 400, 40 and 4 (Table 1). The solutions were filter-sterilised (pore size 0.2 µm) into autoclaved, gas tight and N₂-filled serum bottles and later injected into the bottles using gas-tight syringes. The microcosms were destructively sampled at

seven timepoints, T0-T6: 0 with no resources added, 2, 4, 7, 14, 21 and 40 days after adding the resources.

Table 1: Experiment set up with fertilisation treatments, carbon and nitrate equivalents in kilogram per hectare and the carbon:nitrate ratios.

Treatment	Carbon equivalent	Nitrate-N equivalent	C:NO₃⁻ ratio
C1:N1	8000kg/ha	200kg/ha	40
C1:N2	8000kg/ha	20kg/ha	400
C2:N1	800kg/ha	200kg/ha	4
C2:N2	800kg/ha	20kg/ha	40

The full experimental set-up was composed of five treatments, four resource levels and one negative control, seven timepoints and three replicates arranged in randomised blocks. Timepoint 0 was untreated, hence, there were $5 \times 6 + 1 = 31$ groups and 93 microcosms in total.

The sampling was done by first sampling the gas headspace, using needles and syringes to mix and draw out 5 mL samples of gas, which were injected into capped Gas Chromatograph vials. For timepoints T1-T3 that were from previous experiment results expected to have high N₂O concentration additional 1 mL samples were taken (Fig. 3A). The bottles were then opened to take a 5 g sample for nitrogen extractions and two 1.5 ml Eppendorf tubes of soil for DNA extraction. All soil samples were kept at -20° C until analysis.

2.3 Assessing microbial functional guilds

2.3.1 DNA extraction

DNA was extracted from 350-400 mg soil samples (fresh weight) using the NucleoSpin® Soil kit Genomic DNA from soil. The quality and quantity of the extracted DNA were evaluated using both Nanodrop and Qubit, using a Broad range assay kit since the samples, composed of DNA from a full soil microbiome, had a high concentration of DNA. Nanodrop is based on spectrophotometry, measures absorbance, and is used directly on the extract. The peak for double stranded DNA is collected at wavelength 260 nm, as well as at 230 and 280 for extract contaminants. Qubit, on the other hand, measures only, in this case, the double stranded DNA concentration by a collecting fluorescence signal from an

added dye. This gives a more accurate DNA measurement but does not provide quality measurements.

The extracts were diluted with ultrapure water to a concentration of 1ng/ μL to maximize the change for and equal amplification conditions across all samples at later qPCR marker gene quantification.

2.3.2 Quantitative PCR of marker genes

Quantitative real-time PCR, qPCR, utilizes amplification of genetic material along with spectrophotometry and collected absorbance of DNA, as it is bound to an added dye to quantify the gene copies after every PCR cycle. This, when run together with standards of known concentrations of the targeted gene, it is possible to calculate the number of copies of the gene present in the sample. It can thus be used to estimate the quantity of a gene, species or group in a sample.

However, quantifying the number of functional gene copies only assesses the genetic potential but not the corresponding gene expression or enzymatic activity. It has been shown that measured genetic potential can misrepresent the actual functionality in a sample (Rocca et al. 2015). The method thus reflects the genetic potential for a process in a community (Yoon et al. 2015; Putz et al. 2018; Heo et al. 2020).

First, an inhibition test with pCR[®]4 TOPO[®] plasmids was performed to rule out that inhibiting factors in the extracts were affecting the amplification. Because of a slight inhibition with 4 ng DNA per reaction, 3 ng DNA per reaction was used. Primers for *nirK*, *nirS*, *nrfA*, 16S rRNA and M13 plasmid were diluted to concentrations of 15 μM , 30 μM , 32 μM , 15 μM and 15 μM respectively (Tables 2-6). This was done with Low EDTA TE (1X) pH 8.0 to chelate metal ions to inhibit DNase and prevent DNA degradation (<https://www.qualitybiological.com/product/low-edta-te-1x-ph-8-0/>). Per reaction, 12 μL mastermix made with iQ[™] SYBR[®] Green Supermix, was run with 3 μL sample in two Biorad CFX Connect qPCR machines according to the respective protocol for each primer pair (Table 2-6). Along with the samples there were two replicates of six different standards (0.5×10^7 - 0.5×10^2 copies per reaction) and four negative controls with ultrapure water was run using the same volumes. The standards were prepared by diluting a 4 μL pre-made standard of 0.5×10^9 copies per μL , first to 0.5×10^8 copies/ μL by adding 36 μL ultrapure water. Then 4 μL were transferred into new 200 μL tubes with 36 μL ultrapure water stepwise to make standards 0.5×10^7 - 0.5×10^2 copies. The tubes were mixed between the steps by vortexing. The efficiency of each run is presented in Tables 3-6. The C_q values of the standards were used to create a linear standard curve for determining the number

of copies of the targeted gene in the different samples. Two independent runs of the same marker gene were compared, when the Cq ratio between the runs was outside of 1.1-0.9 the samples were rerun.

At one of the two runs a melting curve measurement was added. It measures at which temperature the DNA strands dissociate, which depends on the nucleotide sequence length and composition. If the curve of the standards matches that of the samples, this indicate that the targeted gene in the samples are so similar that the amplification rate of the standards are comparable with that of the samples. As a second quality check, the PCR products from the run without melting curve were run on gel to see that the bands were clear, of similar size to each other, and to a standard and that no bands were visible from the water controls. The gels were made with Sodium Borate (SB) buffer providing high resolution and short running time (Brody & Kern 2004), 1% agar and 1.5 μ L Nancy red dye per 50 ml buffer. The PCR products were mixed with 5 μ L loading buffer and 5 μ L where then loaded onto the gel. It was run in SB buffer at 200 volt and 400 milli ampere for 20 minutes.

Table 2: Inhibition test with pCR[®]4 TOPO[®] plasmid (DNASU 2022) for qPCR quantification with primers, master mix composition in concentrations per reaction and protocol.

Primers	M13R GTAAAACGACGGCCAG M13F CAGGAAACAGCTATGAC
Mastermix concentration per reaction	0.25 μ M M13R, 0.25 μ M M13F, 0.1% BSA, 1x iQ [™] SYBR [®] Green Supermix, 3 ng/rx DNA sample
Volume	15 μ L, 3 μ L sample
Protocol	(95°C 5min) x 1 (95°C 15s, 55°C 30s, 72°C 30s, 80°C 5s) x 35 Fluorescence is collected at 80°C.

Table 3: qPCR quantification of 16S rRNA marker gene with primers, master mix composition in concentrations per reaction and protocol by (Parada et al. 2016), as well as the efficiency of the conducted qPCR run.

Primers	515F GTGYCAGCMGCCGCGGTAA 926R CCGYCAATTYMTTTRAGTT.
Mastermix concentration per reaction	0.5 μ M 515F, 0.5 μ M 926R, 0.1% BSA, 1x iQ [™] SYBR [®] Green Supermix, 3 ng/rx DNA sample
Volume	15 μ L, 3 μ L sample
Protocol	(95°C 5 min) x 1 (95°C 15s, 50°C 30s, 72°C 30s, 78°C 5s) x 35 Fluorescence is collected at 78°C. Melt curve 95°C for 10s followed by 65 °C - 95 °C (5s increment 0,5 °C)
Efficiency	86-101%

Table 4: qPCR quantification of *nirK* marker gene with primers, master mix composition in concentrations per reaction and protocol by (Throbäck et al. 2004), as well as the efficiency of the conducted qPCR run.

Primers	876F 1040R
Mastermix concentration per reaction	0.5 µM nirK 876F, 0.5 µM nirK 1040R, 15 µg BSA, 1x iQ™ SYBR® Green Supermix, 3 ng/rx DNA sample
Volume	15 ul, 3ul sample
Protocol	(95°C 5 min) x 1 (95°C 15s, (63-58°C -1°/cycle) 30s, 72°C 30s) x 6 (95°C 15s, 58°C 30s, 72°C 30s, 80°C 5s)x35 (95°C 15s) x 1 Fluorescence is collected at 80°C. Melt curve 65 °C - 95 °C (5s increment 0,5 °)
Efficiency	74-94%

Table 5: qPCR quantification of *nirS* marker gene with primers, master mix composition in concentrations per reaction and protocol by (Throbäck et al. 2004), as well as the efficiency of the conducted qPCR run.

Primers	Cd3aFm AACGYSAAGGARACSGG R3cdm GCCTCGATCAGRTRTGGTT
Mastermix concentration per reaction	0.5 µM, Cd3aFm, 0.5 µM R3cdm, 0.1% BSA, 1x iQ™ SYBR® Green Supermix, 3 ng/rx DNA sample
Volume	15 ul, 3ul sample
Protocol	(95°C 5 min) x 1 (95°C 15s, (65-60°C -1°/cycle) 30s, 72°C 30s) x 6 (95°C 15s, 60°C 30s, 72°C 30s, 80°C 5s) x 35 (95°C 15s) x 1 Fluorescence is collected at 80°C. Melt curve 60 °C - 95 °C (10s increment 0,5 °C)
Efficiency	60-86%

Table 6: qPCR quantification of *nrfA* marker gene with primers, master mix composition in concentrations per reaction and protocol by (Cannon et al. 2019), as well as the efficiency of the conducted qPCR run.

Primers	NrfAF2awMOD NrfAR1MOD
Mastermix concentration per reaction	2 μ M NrfAF2awMOD, 2 μ M NrfAR1MOD, 15 μ g BSA, 1x iQ™ SYBR® Green Supermix, 3 ng/rx DNA sample
Volume	15 ul, 3ul sample
Protocol	(95°C 5 min) x 1 (95°C 30s, 56°C 30s, 72°C 30s, 80°C 5s) x 35 (95°C 15s) x 1 Fluorescence is collected at 80°C. Melt curve 65 °C - 95 °C (5s increment 0,5 °C)
Efficiency	55-68%

To calculate gene copies/g dry weight soil the intercept of the standard curve was subtracted from the mean value of C_q value from the two runs and divided by the slope of the curve. This was then multiplied by the factor each sample was diluted with to achieve the 1 ng/ μ L that was used for the reactions, multiplied with the elution volume and divided by the soil sample weight corrected to dry weight by dividing the moisture content.

For the results *nirK* and *nirS* were combined and described simply as *nir*. The relative abundance *nir* and *nrfA* was calculated by dividing their gene copies/g dry weight soil with the number of 16S rRNA gene copies/g dry weight soil. This was done to estimate the proportions of the microbial community that possess the genetic potential for denitrification and DNRA. In addition, a ratio between the two groups was calculated by dividing one of their gene copy number/g dry weight soil with that of the other.

2.1 Ammonium and nitrate measurements in soil samples

2.1.1 Ammonium- and nitrate-nitrogen extraction

To the 5 g frozen soil samples 20 ml of 2 M potassium chloride solution (KCl) was added into falcon tubes and shaken for 1h at 300 rotations per minute (rpm). The tubes were then centrifuged for 5 at 4300 rpm and then filtered into new falcon tubes through funnels with filter paper previously leached with 5 ml 2M KCl. Blank samples were made in the same way as the soil extracts but without any soil. The final extracts were kept at -20° C until analysis.

2.1.2 Analysis with SEAL AutoAnalyzer 500

SEAL AutoAnalyser 500 is an automatic spectrophotometric analyser that measures NH_4^+ concentration in an extract by measuring the absorbance of it when mixed with dyeing reagents. It also measures NO_3^- by first reducing it to NO_2^- in a copper-cadmium coil to then measure colour reaction as it is mixed with reagents.

Reagents for NO_3^- and NH_4^+ analysis and standard stock solutions were prepared according to SEAL Analytical Method no. A-044-19 Rev. 3 and Method no A-048-19 Rev 1 respectively (Appendix 1). Extracts from left over soil were prepared to test a set of NO_3^- and NH_4^+ standards that covers the range of NO_3^- and NH_4^+ in the soil.

For the sample analysis two sets of standards were used, one high range and one low range. The NH_4^+ concentrations were however the same for the low and high range: 7.5, 4, 2.5, 1.5, 0.75, 0.3, and 0.1 mg/L since we deemed it would cover the variation among the samples. The high range NO_3^- standards were of the same concentrations as the NH_4^+ standards while the low range NO_3^- standards were of concentrations: 0.75, 0.4, 0.25, 0.15, 0.075, 0.03, and 0.01 mg/L. All standards were made by diluting stock solutions with 2M KCL, they were prepared and poured into SEAL analysis tubes, as were the soil extracts after thawing and 3s of vortexing. The analysis was done according to the protocols (Appendix 1). For extracts with NO_3^- concentrations that were out of range, they were kept at 4° C, diluted by a factor of 30 with 2M KCl and then run again.

The analysis output in mg/L were corrected by subtracting the average blank value and calculated to mg/kg dry weight soil by multiplying it with the extraction volume 0.2 L. This was divided by the soil sample weight corrected to dry weight by dividing the moisture content. Finally, it was multiplied by 1000 to get mg/kg dw soil.

2.1 Nitrous oxide measurements

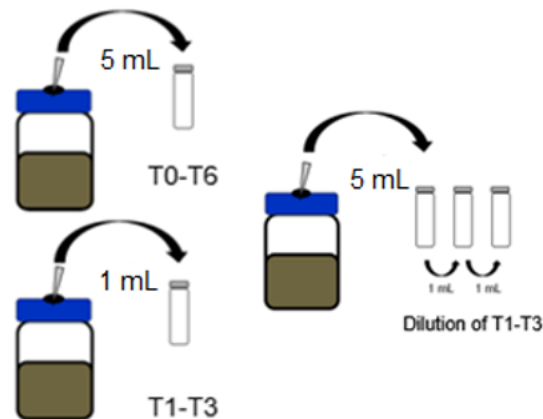
2.1.1 Gas chromatography

The 5 mL 22.5 mL GC sample vials and the 1 mL sample vials of T1, T2 and T3 were run to measure N_2O concentration in the vials. Because the 1 mL samples were out of range for T1-T3, the 5 mL gas samples of the corresponding microcosms were used to make diluted samples. This was done by transferring 1 mL to a dilution vial of 22.5 mL and from that vial 1 ml was transferred to another

22.5 mL GC vial which was used for analysis. Five air samples were run along the with the sample to check air background baseline.

Two sets of 9 standards with the N₂O concentrations 3.57, 7.12, 17.80, 70.62, 105.48, 171.52, 510.26, 846.70 and 1692.05 ppm were prepared in serum bottles where the air had been exchanged with N₂. Five mL of these standards were injected into GC vials and run along with five air samples. The first 1 mL samples of timepoint T1-T3 that were out of range were diluted to where 1 mL was used as the injection volume, why they had to be compared to standards with the same injection volume. For this reason, a second group of standards were prepared with 1 mL injection volume and run, also together with five air samples. The results were used to make two standard curves. The replication of the standards, put before and after the samples in the vial carousel, was used to check for any drift in the run. The air samples were used to check the background air N₂O concentration in the air, since the atmosphere in the GC sample vials were not replaced with N₂.

A



B

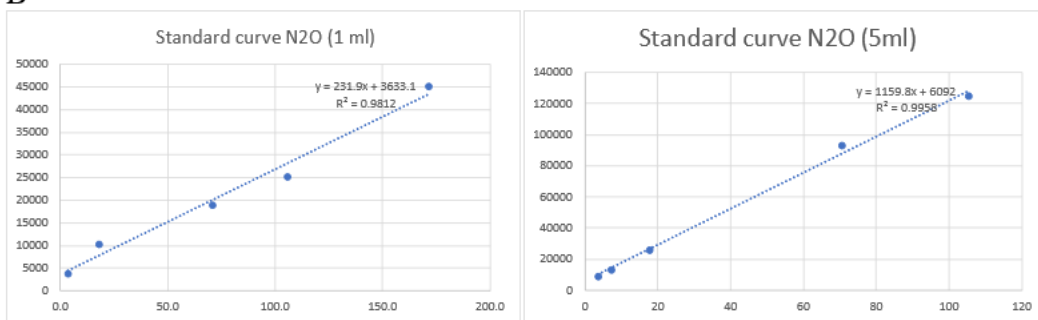


Figure 3: Gas sampling of microcosm headspaces and standard curves for calculating N₂O concentrations. A) Sampling of the microcosm headspaces for the different timepoints: T0-T6; 0, 2, 4, 7, 14, 21 and 40 days after the addition of resources, and dilution of samples from timepoints T1-T3. B) Gas chromatography standard curves made with 1 mL and 5 mL volumes with the N₂O concentrations: 3.57, 7.12, 17.80, 70.62, 105.48, 171.52, 510.26, 846.70 and 1692.05 ppm for calculation of the N₂O concentrations in the samples. Shows equation and R² of the curves.

To calculate the N₂O concentration in ppm the samples, the 5 mL taken from the microcosm headspace diluted into 22.5 mL air in a GC vial, from peak area the intercept of the standard curve was subtracted from peak area value and divided by the slope of the curve (Fig. 3B). This was then corrected by the dilution factor, for the undiluted samples and for the diluted. This does not reflect the actual N₂O concentration in the microcosm headspace, it does only make all the samples comparable so that their relationship to each other may be studied.

2.2 Data analysis

The raw data was analysed using the 4.1.1 version of the R Studio program (R Core Team 2020). The data was first tested for homogeneity, normality and independence using the Levene's test, the Shapiro-Wilk test and the Durbin-Watson test respectively. Since the data did not follow a normal distribution, the non-parametric Kruskal-Wallis test was used to test if there were any significant differences between groups. The Kruskal-Wallis test with multiple comparison, as built in to the "agricolae" package (version 1.4-5), uses as post-hoc test Fisher's least significant difference. This test was used for all the measurements to compare groups of treatment-timepoint combination with each other for significant differences, $p < 0.05$. Boxplots were created with group, as factor using the "ggplot2" package (version 3.3.6). Significance was tested between all the 31 groups for each measurement. To disentangle the effect of treatment with added C and NO₃⁻ resources from the effect of incubation time, another Kruskal-Wallis test with multiple comparison tested by Fisher's least significant difference was done on the data separated by timepoint, testing for differences between C and NO₃⁻ treatments (Table 1). This tests for significance between all C and NO₃⁻ treatments at a given timepoint.

Correlations between the variables were tested. As the data were not normally distributed the non-parametrical Spearman's correlation test was used in the program R, using the package "psych" (version 2.2.5) to do the test, p-value adjustment was done with the default "fdr" method, and the package "ggpubr" (version 0.4.0) was used to visualise the correlations with scatterplots. This was done between the different nitrogen measurements, NO₃⁻, NH₄⁺ and N₂O, between them and the gene copies of each marker gene as well as with a ratio between the number of *nrfA* and *nir* copies. The *nir* and *nrfA* copies were also both compared to the number of 16S rRNA copies. The relative abundance of *nir* and *nrfA*, as calculated by division with the number 16S rRNA copies, were also compared to each other. Additionally, to try to separate ammonium production by DNRA from mineralisation of nitrogen as carbon resources deplete NH₄⁺ concentration was also compared to the relative abundances of *nir* and *nrfA*.

3. Results

This section presents the results of qPCR with functional marker genes, gas chromatography and spectrophotometric analysis of soil extracts. These measurements were taken over the five treatments presented in Table 1, over seven timepoints, T0-T6: 0 with no resources added, 2, 4, 7, 14, 21 and 40 days after adding the resources. The results are presented for 31 groups given by the treatment and timepoints. For clarity, “group” in this section refer to the combinations of treatment and timepoint.

3.1 Soil nitrogen content

At T1, NO_3^- concentrations in the soil extracts were highest in the high *C1:N1* treatment, followed by *C2:N1* and *C1:N2* (Figure 4). In the two latter, they were below detection level 4 days after the addition of resources. In *C1:N1*, all the NO_3^- was consumed between day 4 and 7. There were no detectable amounts of NO_3^- at T0, nor in the *C2:N2* and control treatments for any of the time points.

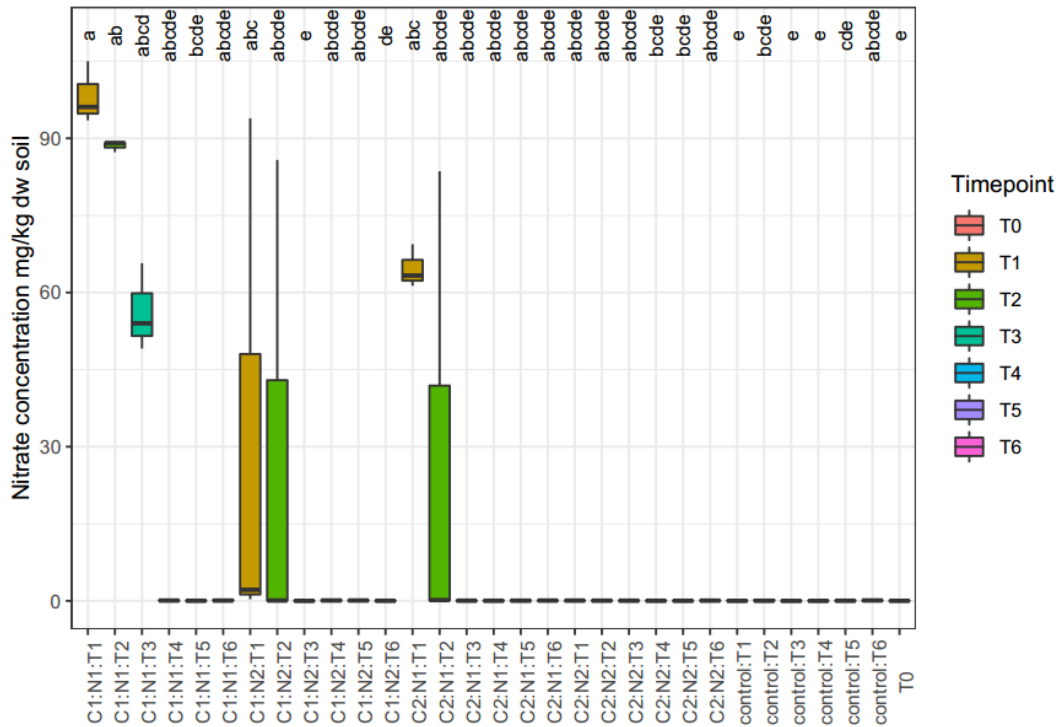


Figure 4: Nitrate concentrations in soil extracts (2M potassium chloride) across the different treatments: C1: 8000 kg C/ha, C2: 800 kg C/ha, N1: 200 kg NO₃-N/ha, N2: 20 kg NO₃-N/ha and timepoints T0-T6; 0, 2, 4, 7, 14, 21 and 40 days after the addition of resources. No resources were added in the control bottles. The hinges of the boxes, upper and lower, correspond to the 75th and 25th percentiles respectively. The whiskers represent the min and max values but excludes outliers, the lines through the boxes represent the medians. Significant differences between the groups, tested with Kruskal-Wallis test followed by Fisher's least significant difference, are indicated by letters, adjusted p-value < 0.05.

For comparisons within timepoints, *C1:N1* was significantly higher from *C1:N2*, *C2:N2* and control, but not from *C2:N1* for timepoint T1 (Table 7). This was also the case for timepoint T2, except for that *C1:N2* is not significantly different from *C1:N1*. Similarly, timepoint T3 showed the same pattern as T1, except for that *C2:N2* is no longer significantly different from any other treatment but the control. The treatment comparisons of timepoints T4, T5 and T6 showed no significant differences.

Table 7: Statistical analysis of differences in nitrate concentration across the different treatments: C1: 8000 kg C/ha, C2: 800 kg C/ha, N1: 200 kg NO₃⁻-N/ha, N2: 20 kg NO₃⁻-N/ha for each timepoint: T0-T6; 0, 2, 4, 7, 14, 21 and 40 days after the addition of resources. Significance was tested with Kruskal-Wallis test followed by Fisher's least significant difference, and is indicated by the letters, adjusted p-value < 0.05. Note that the letter-groups are attributed to each treatment tested within a given timepoint, the table should thus only be read by column and not by row.

NO₃⁻	T1	T2	T3	T4	T5	T6
C1:N1	a	a	a	a	a	a
C1:N2	b	ab	b	a	a	a
C2:N1	ab	ab	ab	a	a	a
C2:N2	c	b	ab	a	a	a
control	c	b	b	a	a	a

Regarding NH₄⁺, there was a trend of increasing concentration after 7 days, at T3, across all treatments (Fig. 5). For all treatments but the control the NH₄⁺ concentration initially decreased from T0 to T2 for ratio *C1:N1*, *C2:N1* and *C2:N2*, and from T0 until T3 for *C1:N2*. The magnitude and range of this trend did also vary between the ratios, *C1:N1* and *C2:N1* started out as the lowest and ended with the highest NH₄⁺ concentrations. *C1:N2* and *C2:N2* started with higher concentrations and ended with lower concentrations compared to the other two ratios. It also seemed that the highest variance within groups is found at timepoint T6.

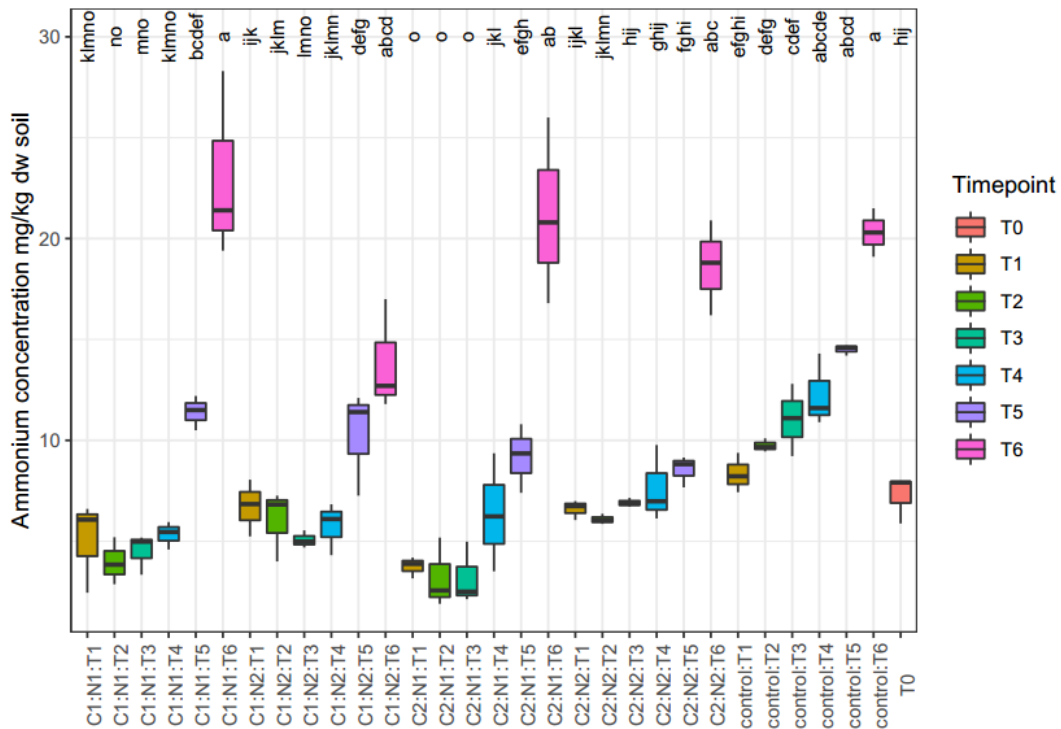


Figure 5: Ammonium concentration in soil extracts (2M potassium chloride) across the different treatments: C1: 8000 kg C/ha, C2: 800 kg C/ha, N1: 200 kg NO₃⁻-N/ha, N2: 20 kg NO₃⁻-N/ha and timepoints T0-T6; 0, 2, 4, 7, 14, 21 and 40 days after the addition of resources. No resources were added in the control bottles. The hinges of the boxes, upper and lower, correspond to the 75th and 25th percentiles respectively. The whiskers represent the min and max values but excludes outliers, the lines through the boxes represent the medians. Significant differences between the groups, tested with Kruskal-Wallis test followed by Fisher's least significant difference, are indicated by letters, adjusted p-value < 0.05.

For comparisons within timepoints where the only significant differences were between the control treatment, that was higher, and the treatments *C1:N1* and *C2:N1* at T1 (Table 8). For timepoint T2 the treatments *C1:N1* and *C2:N1* were not significantly different from the control. At T3, the only significant differences were between *C1:N1*, *C1:N2* and *C2:N1* that were higher than *C2:N2* and control. For timepoint T4 *C1:N1* and *C1:N2* were significantly lower than the control. At timepoint T5 were *C2:N1* and *C2:N2* the only treatments that were significantly different from the others, they were lower than the others but not significantly different from each other. There were no significant differences among treatments at timepoint T6.

Table 8: Statistical analysis of differences in ammonium concentration across treatments: C1: 8000 kg C/ha, C2: 800 kg C/ha, N1: 200 kg NO₃⁻-N/ha, N2: 20 kg NO₃⁻-N/ha for each timepoint: T0-T6; 0, 2, 4, 7, 14, 21 and 40 days after the addition of resources. Significance was tested with Kruskal-Wallis test followed by Fisher's least significant difference, and is indicated by the letters, adjusted p-value < 0.05. Note that the letter-groups are attributed to each treatment tested within a given timepoint, the table should thus only be read by column and not by row.

NH₄⁺	T1	T2	T3	T4	T5	T6
C1:N1	b	bc	b	b	ab	a
C1:N2	ab	ab	b	b	ab	a
C2:N1	b	c	b	ab	b	a
C2:N2	ab	ab	a	ab	b	a
control	a	a	a	a	a	a

3.2 Nitrous oxide

Analysis of microcosm gas headspace samples showed N₂O concentrations below the detection limit for all treatments at the timepoints T4-T6, as well as for T0 (Fig. 6). For the *C1:N1* treatment the N₂O concentrations started off with detectable amounts at timepoint T1 and increased through T2 to T3. There was, however, high variance at T3. For the *C1:N2* treatment the N₂O concentrations were comparable to that of *C1:N2* at T1 and then increased for T2 and decreased at T3. For the *C2:N1* treatment the N₂O concentrations were higher at T1 compared to *C1:N1* and *C1:N2* and then increased for T2, however with high variance, and is below detection level at T3. For the *C2:N2* treatment the N₂O concentrations were comparable to that of *C1:N1* and *C1:N2* at T1, from there it decreased to below detection level.

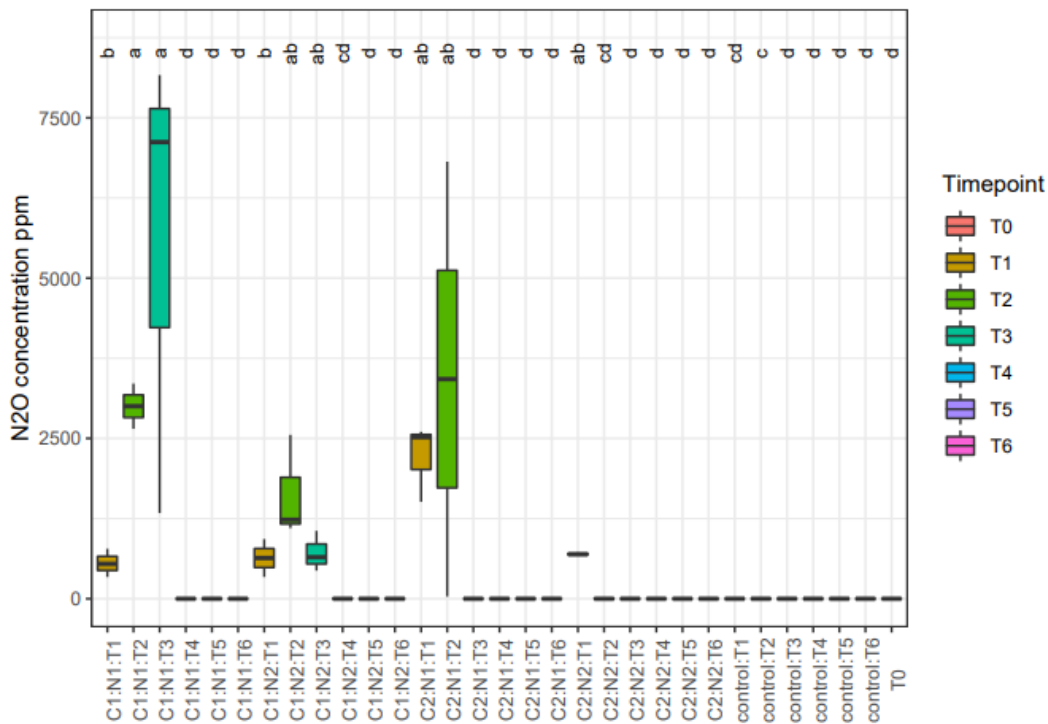


Figure 6: Nitrous oxide concentration from gas headspaces in incubated bottles with soil across the different treatments: C1: 8000 kg C/ha, C2: 800 kg C/ha, N1: 200 kg NO₃⁻-N/ha, N2: 20 kg NO₃⁻-N/ha and timepoints T0-T6; 0, 2, 4, 7, 14, 21 and 40 days after the addition of resources. No resources were added in the control bottles. The hinges of the boxes, upper and lower, correspond to the 75th and 25th percentiles respectively. The whiskers represent the min and max values but excludes outliers, the lines through the boxes represent the medians. Significant differences between the groups, tested with Kruskal-Wallis test followed by Fisher's least significant difference, are indicated by letters, adjusted p-value < 0.05.

When comparing within time points, there were significant differences between the control treatment and all other treatments as well as between C2:N1 and all other treatments for timepoint T1 (Table 9). For timepoint T2 treatments C1:N1, C1:N2 and C2:N1 were significantly different from C2:N2 and the control treatments. At timepoint T3 C1:N1 and C1:N2 were significantly different from the other treatments, and also from each other. The following timepoint T4-T6 showed no significant differences between the treatments.

Table 9: Statistical analysis of differences in net nitrous oxide production across the different treatments: C1: 8000 kg C/ha, C2: 800 kg C/ha, N1: 200 kg NO₃⁻-N/ha, N2: 20 kg NO₃⁻-N/ha for each timepoint: T0-T6; 0, 2, 4, 7, 14, 21 and 40 days after the addition of resources. Significance was tested with Kruskal-Wallis test followed by Fisher's least significant difference, and is indicated by the letters, adjusted p-value < 0.05. Note that the letter-groups are attributed to each treatment tested within a given timepoint, the table should thus only be read by column and not by row.

N₂O	T1	T2	T3	T4	T5	T6
C1:N1	b	a	a	a	a	a
C1:N2	b	a	b	a	a	a
C2:N1	a	a	c	a	a	a
C2:N2	b	b	c	a	a	a
control	c	b	c	a	a	a

3.3 Microbial functional guilds

3.3.1 Bacterial and archaeal abundance

16S rRNA marker gene quantification through qPCR showed timepoint T0 had a high abundance of prokaryotes (Fig. 7) Timepoint T1 and T2 in the *C2:N1* and *C2:N2* ratios, as well as timepoint T1 in the *C1:N2* ratio and T2 and T3 in the *C1:N1* ratio showed similar numbers of gene copies as T0. After that the number of copies is continually decreasing over the following timepoints for all treatments, except for the *C1:N1* ratio. There the copies increase from timepoint T1 until T3, that is slightly higher than at the start at T0. Thereafter it decreases at T4, increases at T5 and finally decrease to its lowest value at T6. The decreasing pattern of ratio *C2:N1* and the control treatment has somewhat of a wider range, i.e. shows a more dramatic change.

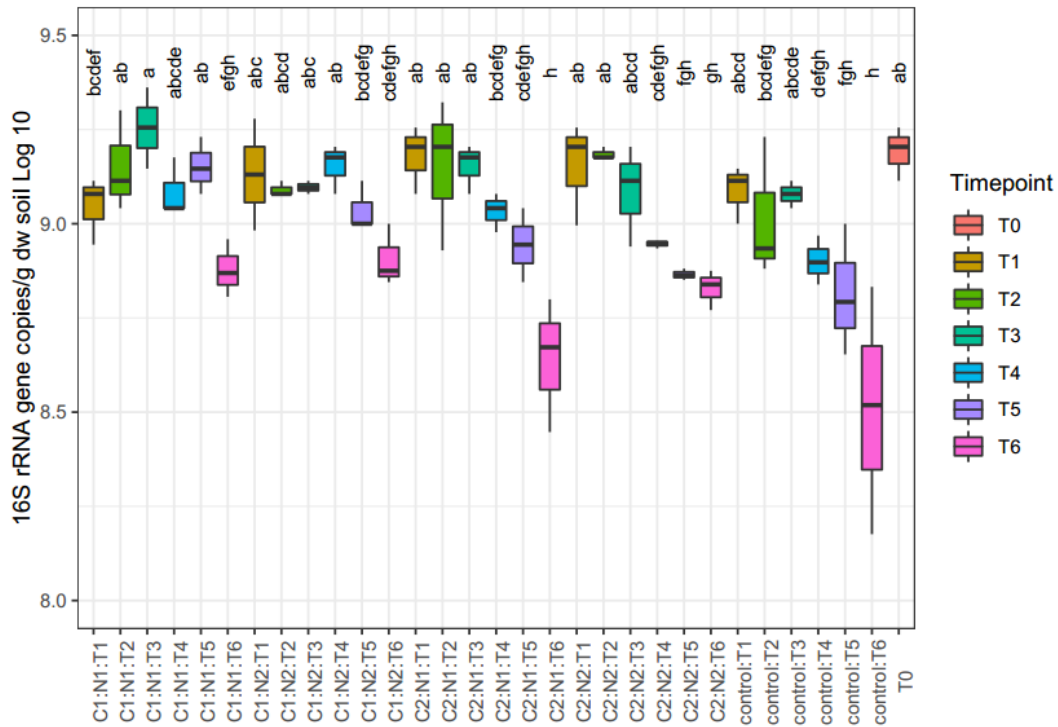


Figure 7: Absolute abundance of the prokaryotic marker gene 16S rRNA in incubated bottles with soil across the different treatments: C1: 8000 kg C/ha, C2: 800 kg C/ha, N1: 200 kg NO₃--N/ha, N2: 20 kg NO₃--N/ha and timepoints T0-T6; 0, 2, 4, 7, 14, 21 and 40 days after the addition of resources. No resources were added in the control bottles. Quantitative PCR of the 16S rRNA marker gene were calculated to gene copies per gram dry weight soil and logged. The hinges of the boxes, upper and lower, correspond to the 75th and 25th percentiles respectively. The whiskers represent the min and max values but excludes outliers, the lines through the boxes represent the medians. Significant differences between the groups, tested with Kruskal-Wallis test followed by Fisher's least significant difference, are indicated by letters, adjusted p-value < 0.05.

When comparing within time points, there were no significant differences between the treatments at T1-T3 (Table 10). At T4 the C2:N2 and control treatments were significantly different from the other treatments. At timepoint T5 the C1:N1 treatment was the only one that showed significant differences to the control treatment, it also showed a significant difference to C2:N2. Lastly at timepoint T6 the C2:N1 and the control treatments showed significant differences to the other treatments.

Table 10: Statistical analysis of differences in absolute abundance of the prokaryotic marker gene 16S rRNA across the different treatments: C1: 8000 kg C/ha, C2: 800 kg C/ha, N1: 200 kg NO₃⁻-N/ha, N2: 20 kg NO₃⁻-N/ha for each timepoint: T0-T6; 0, 2, 4, 7, 14, 21 and 40 days after the addition of resources. Significance was tested with Kruskal-Wallis test followed by Fisher's least significant difference, and is indicated by the letters, adjusted p-value < 0.05. Note that the letter-groups are attributed to each treatment tested within a given timepoint, the table should thus only be read by column and not by row.

16S rRNA	T1	T2	T3	T4	T5	T6
C1:N1	a	a	a	a	a	ab
C1:N2	a	a	a	a	ab	a
C2:N1	a	a	a	a	ab	b
C2:N2	a	a	a	b	b	ab
control	a	a	a	b	b	b

3.3.2 Abundance of denitrifiers

The abundance of *nir* genes, corresponding to the sum of *nirK* and *nirS* copy number, showed that timepoint T0 had a high abundance of denitrifiers (Fig. 8). Timepoint T1 was similarly high for all ratios except for the C1:N1 ratio that had slightly decreased gene copies. Thereafter the gene copy numbers decrease with every timepoint for all ratios but C1:N1 where it instead increases for T1, T2 and T3 to then decrease for T4, increase again for T5 and finally drastically decrease for T6. A drastic decrease between timepoint T5 and T6 was apparent for all treatment but less notable in the C2:N2 ratio. The range of the gene copy numbers between T1 and T6 is slightly wider for C2:N1 and control compared to the other treatments.

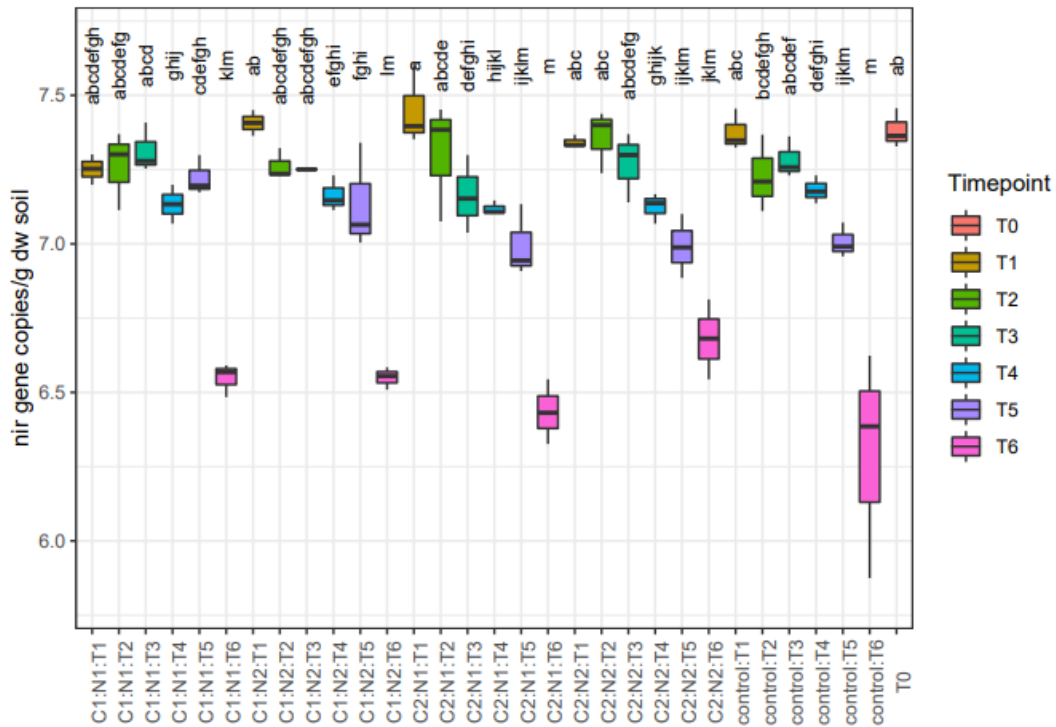


Figure 8: Absolute abundance of the functional marker genes *nirK* and *nirS* in incubated bottles with soil across the different treatments: C1: 8000 kg C/ha, C2: 800 kg C/ha, N1: 200 kg NO₃⁻-N/ha, N2: 20 kg NO₃⁻-N/ha and timepoints T0-T6; 0, 2, 4, 7, 14, 21 and 40 days after the addition of resources. No resources were added in the control bottles. Quantitative PCR of the *nir* marker genes were calculated to gene copies per gram dry weight soil and logged. The hinges of the boxes, upper and lower, correspond to the 75th and 25th percentiles respectively. The whiskers represent the min and max values but excludes outliers, the lines through the boxes represent the medians. Significant differences between the groups, tested with Kruskal-Wallis test followed by Fisher's least significant difference, are indicated by letters, adjusted p-value < 0.05.

Kruskal-Wallis test with multiple comparison tested with Fisher's least significant difference for the *nir* absolute abundance between C and NO₃⁻ treatments showed no significant differences (Table 11).

Table 11: Statistical analysis of differences in absolute abundance of the *nir* marker gene across the different treatments: C1: 8000 kg C/ha, C2: 800 kg C/ha, N1: 200 kg NO₃⁻-N/ha, N2: 20 kg NO₃⁻-N/ha for each timepoint: T0-T6; 0, 2, 4, 7, 14, 21 and 40 days after the addition of resources. Significance was tested with Kruskal-Wallis test followed by Fisher's least significant difference, and is indicated by the letters, adjusted p-value < 0.05. Note that the letter-groups are attributed to each treatment tested within a given timepoint, the table should thus only be read by column and not by row.

<i>Nir</i>	T1	T2	T3	T4	T5	T6
C1:N1	a	a	a	a	a	a
C1:N2	a	a	a	a	a	a
C2:N1	a	a	a	a	a	a
C2:N2	a	a	a	a	a	a
control	a	a	a	a	a	a

Quantification of the relative abundance of the functional *nir* marker genes does generally and quite uniformly decrease with time across all the treatments (Fig. 9). All treatments start with similar values as T0 at T1, with a slight increase for *C1:N2* and *C2:N1*, and thereafter very gradually decrease until T6 where all treatments show a dramatic decrease.

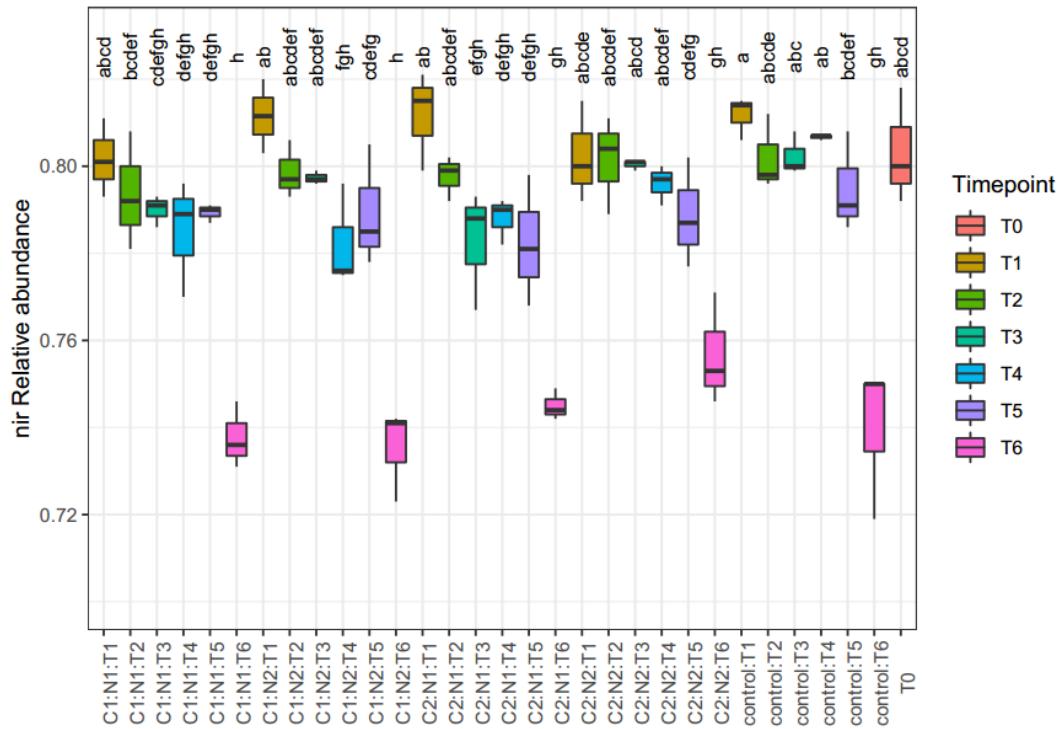


Figure 9: Relative abundance of the functional genes *nirK* and *nirS* in soil across the different treatments: C1: 8000 kg C/ha, C2: 800 kg C/ha, N1: 200 kg NO_3^- -N/ha, N2: 20 kg NO_3^- -N/ha and timepoints T0-T6; 0, 2, 4, 7, 14, 21 and 40 days after the addition of resources. No resources were added in the control bottles. The hinges of the boxes, upper and lower, correspond to the 75th and 25th percentiles respectively. The whiskers represent the min and max values but excludes outliers, the lines through the boxes represent the medians. Significant differences between the groups, tested with Kruskal-Wallis test followed by Fisher's least significant difference, are indicated by letters, adjusted p-value < 0.05.

Kruskal Wallis tests performed on the relative abundance of *nir* between treatments showed significant differences for the timepoints T1, T2, T5 and T6 (Table 12). However, for timepoint T3 *C1:N2* was significantly different from all other treatments, *C1:N1* and *C2:N1* were also different from the *C2:N2* and the control treatments. At timepoint T4 the control treatment was significantly different from all other treatments but *C2:N2*, with no other significant differences between the treatments.

Table 12: Statistical analysis of differences in relative abundance of the *nir* marker gene across the different treatments: C1: 8000 kg C/ha, C2: 800 kg C/ha, N1: 200 kg NO₃⁻-N/ha, N2: 20 kg NO₃⁻-N/ha and timepoints T0-T6; 0, 2, 4, 7, 14, 21 and 40 days after the addition of resources. Significance was tested with Kruskal-Wallis test followed by Fisher's least significant difference, and is indicated by the letters, adjusted p-value < 0.05. Note that the letter-groups are attributed to each treatment tested within a given timepoint, the table should thus only be read by column and not by row.

<i>Nir/16S rRNA</i>	T1	T2	T3	T4	T5	T6
C1:N1	a	a	c	b	a	a
C1:N2	a	a	b	b	a	a
C2:N1	a	a	c	b	a	a
C2:N2	a	a	a	ab	a	a
control	a	a	a	a	a	a

3.3.3 Abundance of DNRA

Quantification of the *nrfA* marker gene through qPCR showed less of a pattern than the other genes and soil N and gas measurements (Fig. 10). The statistical analysis by Kruskal-Wallis tests showed that no group was significantly different to any other group. The y-axis scale also indicates that the overall differences are quite low.

There were, nonetheless, trends that could be observed. For the treatment *C1:N1* the number of gene copies decreased from T0 to T1 to then increase over timepoint T2 and T3, decrease below T1 at T4 and T5 to then reach the lowest number at T6. For *C1:N2*, after a very slight decrease from T0, there is no big differences between timepoint T1 throughout T4. At timepoint T5 and T6 there is a decrease, however with no clear difference between the two and high variance within T5. This treatment has small differences between the timepoints and appears very compact in the graph. For *C2:N1* there is a very slight increase from T0 to T1 but there after no clear differences from T1 to T5, and with high variances at all timepoints but T3. There is thereafter a decrease at T6. For the *C2:N2* treatment the gene copies of T0, T1, T2 and T3, thereafter comes a slight decrease from T3 to T4 and from T5 to T6, also for this treatment the variations within the groups are high. Lastly, for the control treatment the variation within the groups were the highest and timepoints T0, T1, T2, T3 and T4 hardly distinguishable from each other and a slight decrease at T5 and T6.

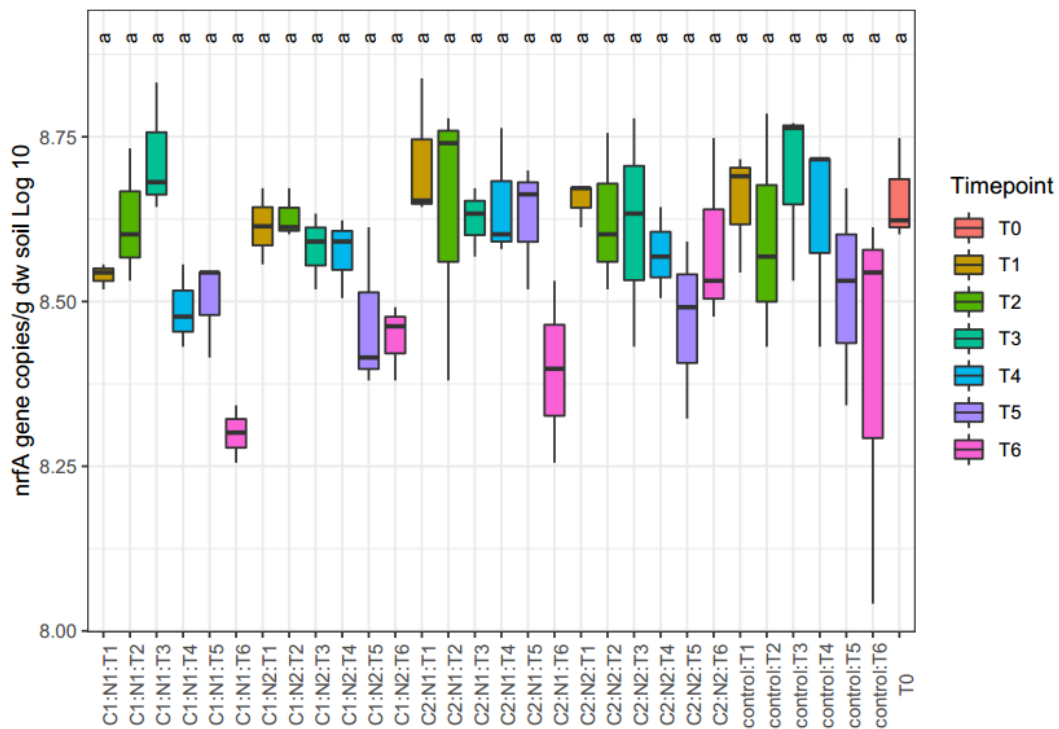


Figure 10: Absolute abundance of the functional marker gene *nrfA* in soil across the different treatments: C1: 8000 kg C/ha, C2: 800 kg C/ha, N1: 200 kg NO₃⁻-N/ha, N2: 20 kg NO₃⁻-N/ha and timepoints T0-T6; 0, 2, 4, 7, 14, 21 and 40 days after the addition of resources. No resources were added in the control bottles. Significant differences between the groups, tested with Kruskal-Wallis test followed by Fisher's least significant difference, are indicated by letters, adjusted p-value < 0.05.

Kruskal Wallis tests on the *nrfA* absolute abundance treatments showed no significant differences (Table 13).

Table 13: Statistical analysis of differences in absolute abundance of the *nrfA* marker gene across the different treatments: C1: 8000 kg C/ha, C2: 800 kg C/ha, N1: 200 kg NO₃⁻-N/ha, N2: 20 kg NO₃⁻-N/ha for each timepoint: T0-T6; 0, 2, 4, 7, 14, 21 and 40 days after the addition of resources. Significance was tested with Kruskal-Wallis test followed by Fisher's least significant difference, and is indicated by the letters, adjusted p-value < 0.05. Note that the letter-groups are attributed to each treatment tested within a given timepoint, the table should thus only be read by column and not by row.

<i>NrfA</i>	T1	T2	T3	T4	T5	T6
C1:N1	a	a	a	a	a	a
C1:N2	a	a	a	a	a	a
C2:N1	a	a	a	a	a	a
C2:N2	a	a	a	a	a	a
control	a	a	a	a	a	a

qPCR quantification of the relative abundance of the functional *nrfA* marker gene shows different trends across the treatments (Fig. 11). For C1:N1 are the timepoints very similar from T0 until T3 and decreases thereafter to T4 and then to T5 to then

increases again for T6. The pattern for *C1:N2* is very similar to that of *C1:N1* but, after the increase at the end from T5, T6 has a higher value than T1. For *C2:N1* T1 is similar to T0, then the values decrease to T2 and T3, however with high variance within T3, to then gradually increase over the timepoints T4, T5 and T6. For *C2:N2* T1 is similar to T0, then the values decrease to T2 to then gradually increase over the timepoints T3, T4, T5 and T6. For the control treatment gradually increase from T0 to T6, maybe with a slight decrease from T4 to T5 but variances within these groups are very high. Timepoint T6 of the control treatment showed the highest value of all the groups.

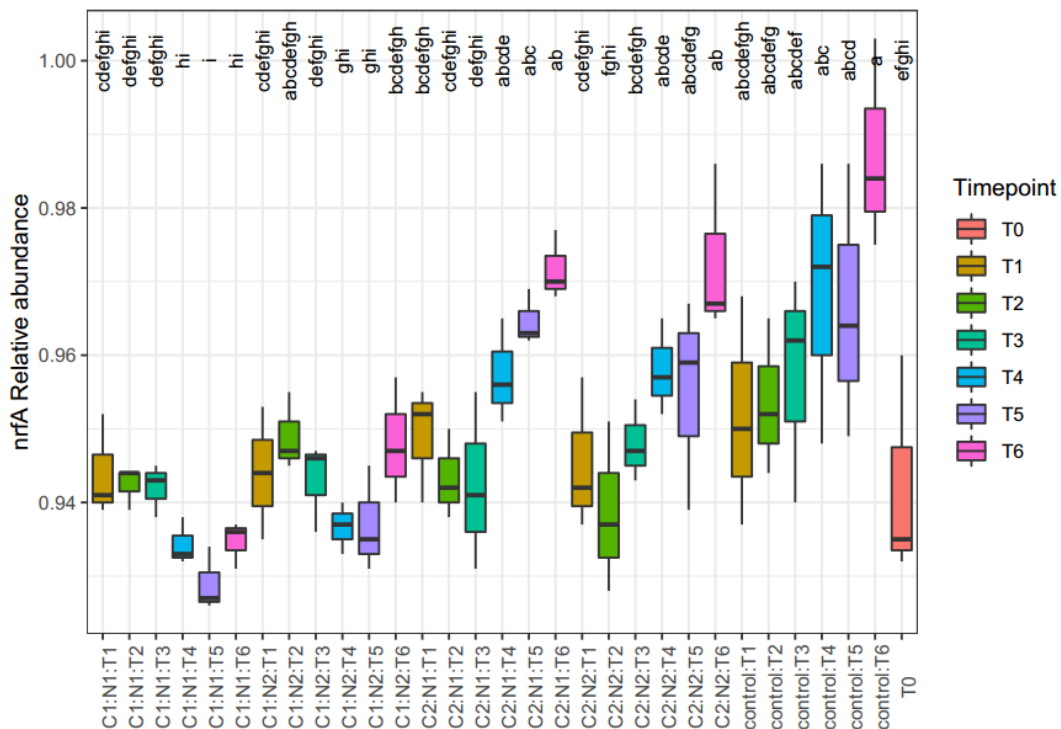


Figure 11: Relative abundance of the functional gene *nrfA* in soil across the different treatments: C1: 8000 kg C/ha, C2: 800 kg C/ha, N1: 200 kg NO₃⁻-N/ha, N2: 20 kg NO₃⁻-N/ha and timepoints T0-T6; 0, 2, 4, 7, 14, 21 and 40 days after the addition of resources. No resources were added in the control bottles. The hinges of the boxes, upper and lower, correspond to the 75th and 25th percentiles respectively. The whiskers represent the min and max values but excludes outliers, the lines through the boxes represent the medians. Significant differences between the groups, tested with Kruskal-Wallis test followed by Fisher's least significant difference, are indicated by letters, adjusted p-value < 0.05.

Kruskal Wallis tests on the relative abundance of *nrfA* between C and NO₃⁻ treatments showed significant differences for the timepoints T1, T2 and T3 (Table 14). However, for timepoint T4 the *C1:N1* and *C1:N2* were significantly different from the other treatments. At timepoint T5 *C1:N1* and *C1:N2* were significantly different from the rest of the treatments, additionally *C2:N1* was significantly different from *C1:N1* and *C1:N2*.

Table 14: Statistical analysis of differences in relative abundance of the *nrfA* marker gene across the different treatments: C1: 8000 kg C/ha, C2: 800 kg C/ha, N1: 200 kg NO₃⁻-N/ha, N2: 20 kg NO₃⁻-N/ha for each timepoint: T0-T6; 0, 2, 4, 7, 14, 21 and 40 days after the addition of resources. Significance was tested with Kruskal-Wallis test followed by Fisher's least significant difference, and is indicated by the letters, adjusted p-value < 0.05. Note that the letter-groups are attributed to each treatment tested within a given timepoint, the table should thus only be read by column and not by row.

<i>NrfA/16S rRNA</i>	T1	T2	T3	T4	T5	T6
C1:N1	a	a	a	b	c	b
C1:N2	a	a	a	b	bc	b
C2:N1	a	a	a	a	a	a
C2:N2	a	a	a	a	ab	a
control	a	a	a	a	a	a

QPCR quantification of the *nrfA/nir* ratio shows similar trends across the treatments with values gradually increasing values from T0 to T5 and a dramatic increase from T5 to T6 (Fig. 12). This pattern is however a bit obscure for the C1:N1 and C1:N2 treatments where there is a decrease from T4 to T5 and at C1:N2 there is also a decrease from T0 to T1. The value of T1 for the C1:N2 treatment was the lowest of the groups and T6 for the control was the highest.

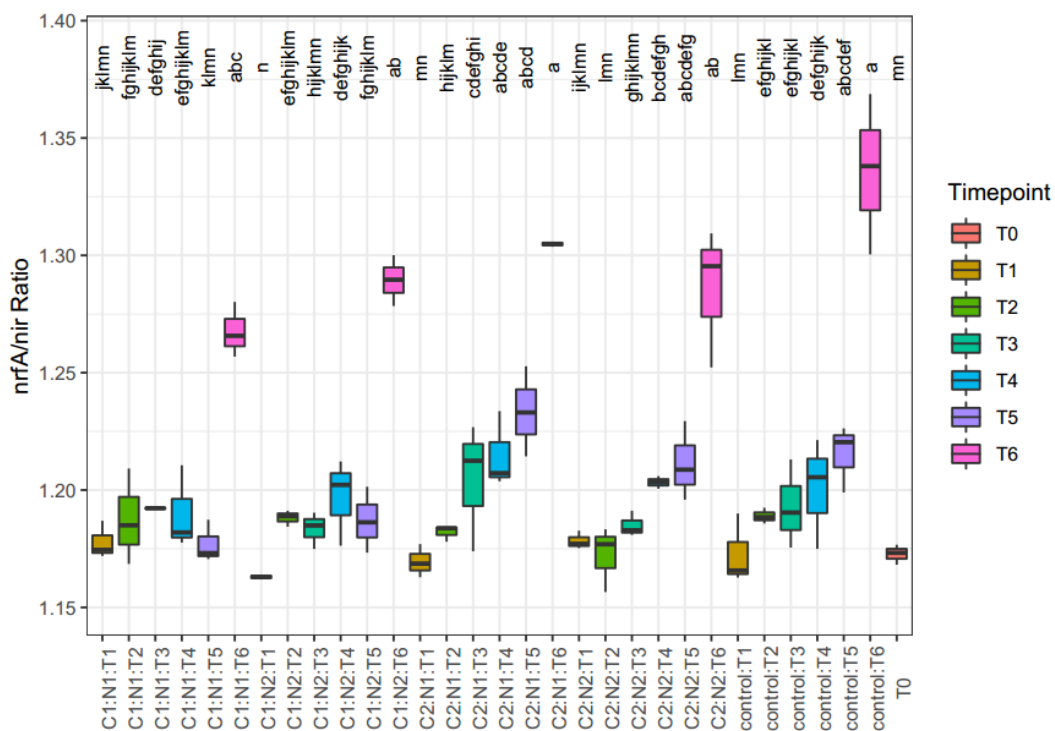


Figure 12: Functional gene *nrfA*/functional *nirK* and *nirS* genes in soil across the different treatments: C1: 8000 kg C/ha, C2: 800 kg C/ha, N1: 200 kg NO₃⁻-N/ha, N2: 20 kg NO₃⁻-N/ha and

timepoints T0-T6; 0, 2, 4, 7, 14, 21 and 40 days after the addition of resources. No resources were added in the control bottles. The hinges of the boxes, upper and lower, correspond to the 75th and 25th percentiles respectively. The whiskers represent the min and max values but excludes outliers, the lines through the boxes represent the medians. Significant differences between the groups, tested with Kruskal-Wallis test followed by Fisher's least significant difference, are indicated by letters, adjusted p-value < 0.05.

Kruskal Wallis tests on the of *nrfA/nir* ratio between C and NO₃⁻ treatments showed significant differences for the timepoints T1, T2, T3, T4 and T6 (Table 15). However, for timepoint T5 the C1:N1 was significantly different from the other treatments but C1:N2.

Table 15: Statistical analysis of differences in relative abundance of *nrfA/nir* ratio across the different treatments: C1: 8000 kg C/ha, C2: 800 kg C/ha, N1: 200 kg NO₃⁻-N/ha, N2: 20 kg NO₃⁻-N/ha for each timepoint: T0-T6; 0, 2, 4, 7, 14, 21 and 40 days after the addition of resources. Significance was tested with Kruskal-Wallis test followed by Fisher's least significant difference, and is indicated by the letters, adjusted p-value < 0.05. Note that the letter-groups are attributed to each treatment tested within a given timepoint, the table should thus only be read by column and not by row.

<i>NrfA/Nir</i>	T1	T2	T3	T4	T5	T6
C1:N1	a	a	a	a	c	a
C1:N2	a	a	a	a	bc	a
C2:N1	a	a	a	a	a	a
C2:N2	a	a	a	a	ab	a
control	a	a	a	a	ab	a

3.4 Correlation study

Spearman's correlation tests between the variables between the different nitrogen measurements, NO₃⁻, NH₄⁺ and N₂O showed a negative moderate significant correlation between NO₃⁻ and NH₄⁺, a strong significant positive correlation between NO₃⁻ and N₂O (Fig. 13), and a strong negative significant correlation

between NH_4^+ and N_2O (Table 16). Correlation between the N pools and the gene copies of each marker gene as well as with a ratio between the number of *nrfA* and *nir* copies was also tested. There were only weak significant correlations between NO_3^- and any of the marker genes. NH_4^+ showed strong significant negative correlations with 16S rRNA and *nir*, a moderate significant negative correlation with *nrfA* and a strong significant positive correlation with the *nrfA/nir* ratio. N_2O showed a moderate significant positive correlation with 16S rRNA and *nrfA* (Fig. 16), a strong significant positive correlation with *nir* (Fig. 15), and a moderate negative significant correlation with the *nrfA/nir* ratio (Fig. 17). The *nir* comparison to 16S rRNA showed the strongest positive significant correlation of the study, closely followed by that of the *nrfA* – 16S rRNA comparison. The comparison between the relative abundance of *nir* and *nrfA*, as calculated by division with the number 16S rRNA copies, showed no significant correlation. NH_4^+ concentration compared to the relative abundances of *nir*, and *nrfA* showed no significant correlation with *nir* relative abundance but and a moderate positive significant correlation for *nrfA* relative abundance (Fig 14).

Table 16: Correlations between variables tested with the Spearman’s correlation test. Rho value indicate the strength of the correlation: 0-0.25 = weak correlation, 0.25-0.5 = moderate correlation, 0.5-0.75 = strong correlation, and adjusted p value indicate the significance: > 0.75 = very strong correlation. N.S for non significant (> 0.05), < 0.05, < 0.01 and < 0.001.

Comparison	Rho	Adjusted p value
$\text{NO}_3^- \sim \text{NH}_4^+$	-0.35	<0.001
$\text{NO}_3^- \sim \text{N}_2\text{O}$	0.51	<0.001
$\text{NH}_4^+ \sim \text{N}_2\text{O}$	-0.61	<0.001
$\text{NO}_3^- \sim 16\text{S rRNA}$	0.23	<0.05
$\text{NO}_3^- \sim nir$	0.18	N.S
$\text{NO}_3^- \sim nrfA$	0.11	N.S
$\text{NO}_3^- \sim nrfA/nir$	-0.14	N.S
$\text{NH}_4^+ \sim 16\text{S rRNA}$	-0.61	<0.001
$\text{NH}_4^+ \sim nir$	-0.55	<0.001
$\text{NH}_4^+ \sim nir/16\text{S rRNA}$	0.1	N.S
$\text{NH}_4^+ \sim nrfA$	-0.33	<0.01
$\text{NH}_4^+ \sim nrfA/16\text{S rRNA}$	0.37	<0.001
$\text{NH}_4^+ \sim nrfA/nir$	0.52	<0.001
$\text{N}_2\text{O} \sim 16\text{S rRNA}$	0.44	<0.001
$\text{N}_2\text{O} \sim nir$	0.52	<0.001
$\text{N}_2\text{O} \sim nrfA$	0.35	<0.001

$N_2O \sim nrfA/nir$	-0.39	<0.001
$nir \sim 16S\ rRNA$	0.79	<0.001
$nrfA \sim 16S\ rRNA$	0.6	<0.001
$nir/16S\ rRNA \sim nrfA/16S\ rRNA$	0.1	N.S

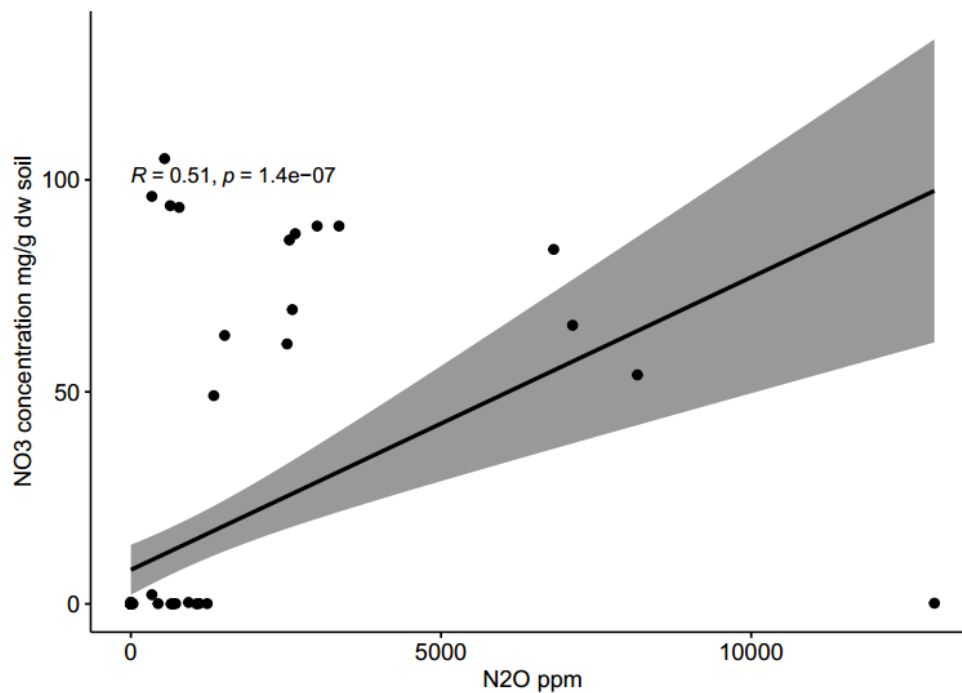


Figure 13: NO_3^- concentration in the incubated soil compared to N_2O concentration in the headspaces of the incubated microcosms was tested with Spearman’s correlation test. It showed a strong positive significant correlation, p- value adjustment was done with the “fdr” method.

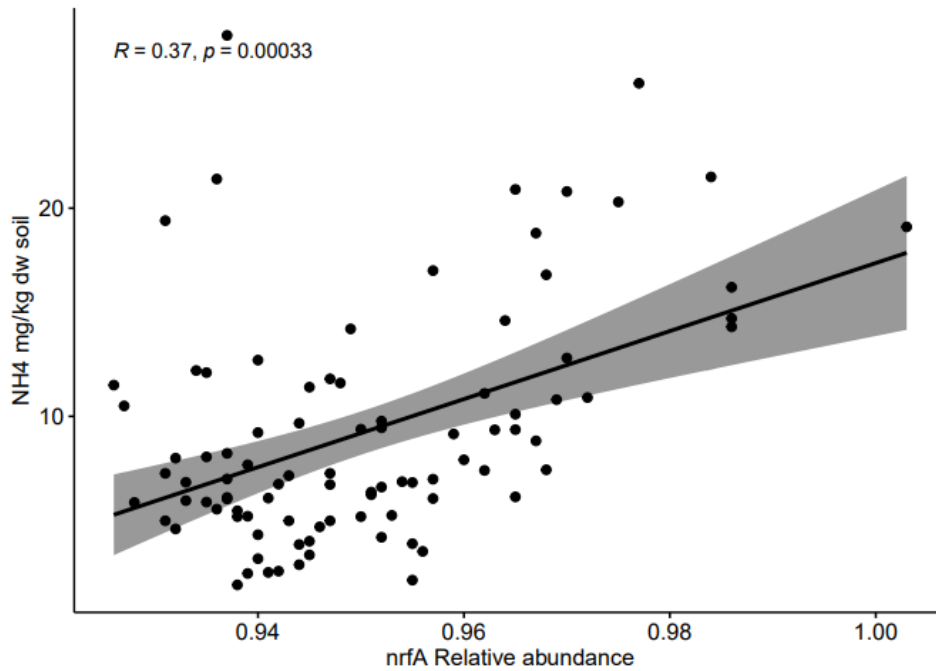


Figure 14: NH_4^+ concentration in the incubated soil compared to the relative abundances of the *nrfA* marker gene concentration in the headspaces of the incubated microcosms was tested with Spearman’s correlation test. It showed a moderate positive significant correlation, p- value adjustment was done with the “fdr” method.

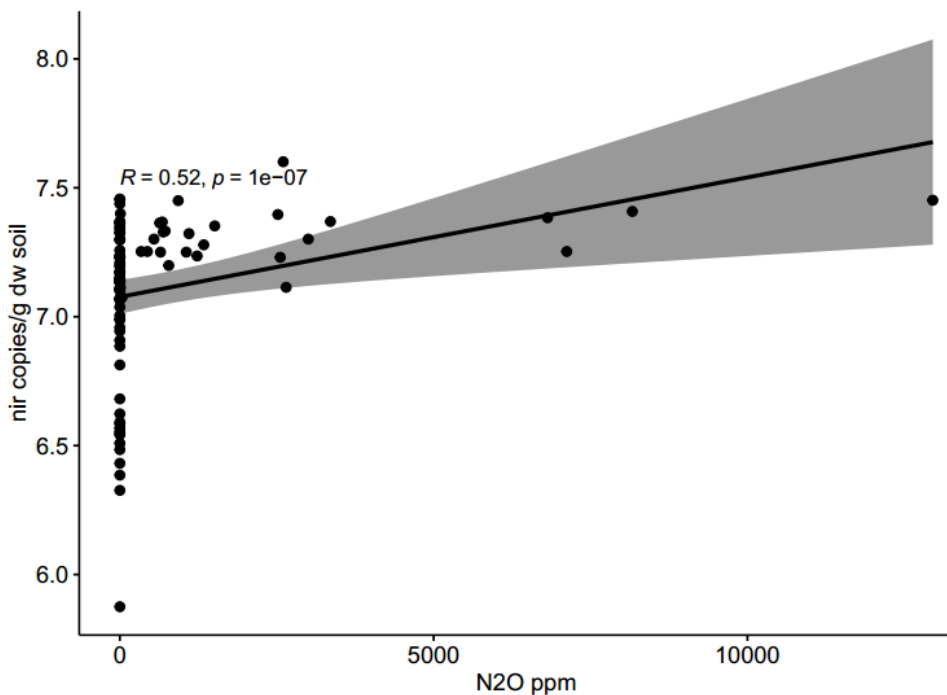


Figure 15: Marker gene *nir* abundance in the incubated soil compared to N_2O concentration in the headspaces of the incubated microcosms was tested with Spearman’s correlation test. It showed a strong positive significant correlation, p- value adjustment was done with the “fdr” method.

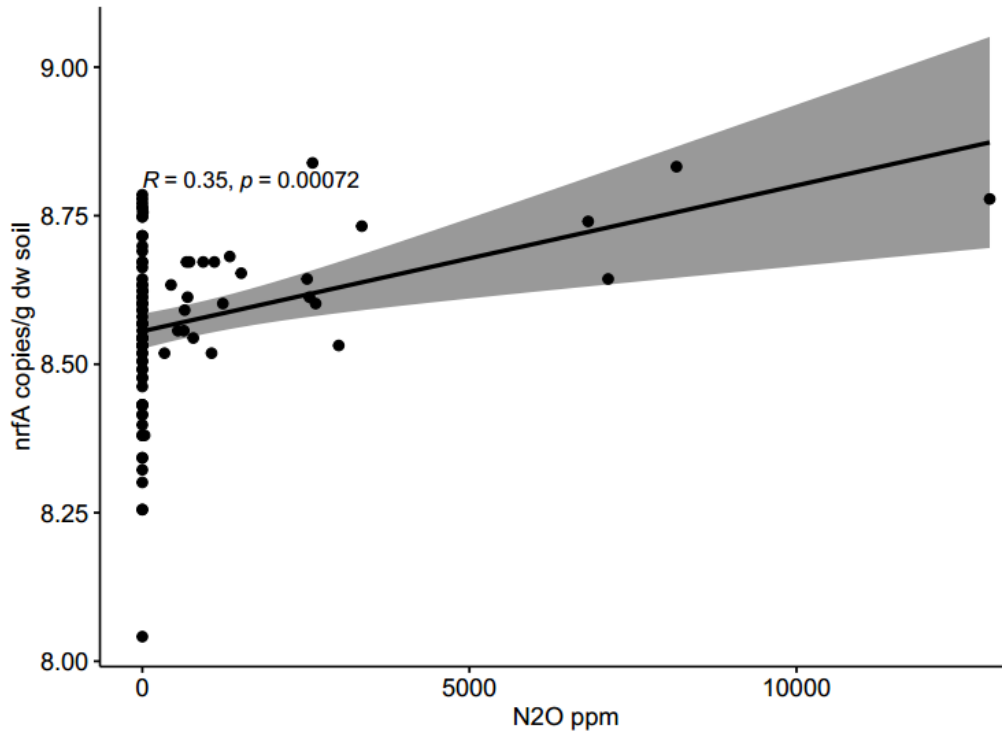


Figure 16: Marker gene *nrfA* abundance in the incubated soil compared to N₂O concentration in the headspaces of the incubated microcosms was tested with Spearman’s correlation test. It showed a moderate significant positive correlation, p- value adjustment was done with the “fdr” method.

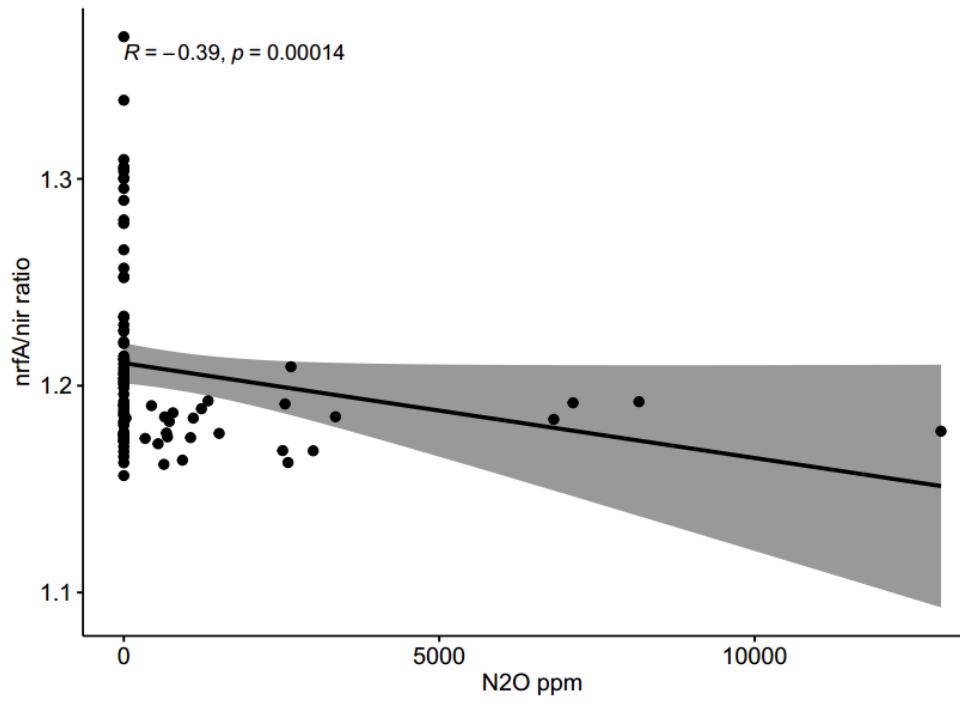


Figure 17: The ratio between marker gene *nrfA/nir* in the incubated soil compared to N₂O concentration in the headspaces of the incubated microcosms was tested with Spearman’s correlation test. It showed a moderate negative significant correlation, p- value adjustment was done with the “fdr” method.

4. Discussion

4.1 Effect of C:NO₃⁻ ratio and amount nitrate respiration pathway over time

The first aim of this experiment was to investigate the effect of different C:NO₃⁻ ratios and amounts on the partitioning of NO₃⁻ between denitrifiers and DNRA measurements on soil nitrogen, net N₂O production and marker genes connected to marker genes for bacterial and archaeal abundance, denitrifier abundance and DNRA abundance.

NO₃⁻ was consumed very fast, no matter the amounts added it was all consumed by timepoint T4, in less than 14 days after addition (Fig 4). There were also very clear differences between the treatments. The *C1:N1* treatment with a C:NO₃⁻ ratio of 40, with a C amount equivalent to 8000 kg/ha and NO₃⁻ amount equal to 200 kg/ha (Table 1) was the slowest to consume its NO₃⁻. This could be expected since it had the highest level of added NO₃⁻. The treatments *C1:N2* with a C:NO₃⁻ ratio of 400, with a C amount equivalent to 8000 kg/ha and NO₃⁻ amount equal to 20 kg/ha and *C2:N1* with a C:NO₃⁻ ratio of 4, with a C amount equivalent to 800 kg/ha and NO₃⁻ amount equal to 200 kg/ha were slower than *C1:N1*. They were also quite similar to each other which was unexpected as *C1:N2* had 10 times less nitrate than *C2:N1*. Perhaps it could be a shortage of easily accessible carbon in *C2:N1* slowing down the respiration.

The treatment *C2:N2* with a C:NO₃⁻ ratio of 40, with a C amount equivalent to 800 kg/ha and a NO₃⁻ amount equal to 20 kg/ha NO₃⁻ consumed all the NO₃⁻ within two days. Although it had the same C:NO₃⁻ ratio as *C1:N1*, the NO₃⁻ was consumed faster, probably because the amount added was 10 times lower. Neither was it similar to *C1:N2* that had the same amount NO₃⁻ but a much higher C:NO₃⁻ ratio and C amount. No amounts of NO₃⁻ could be measured in the control treatment. The treatments with the same amounts of NO₃⁻ consumed it at different rates, perhaps due to a difference in the C:NO₃⁻ ratio or to different C amounts. Something

about high NO_3^- concentration compared to C concentration and/or relatively low carbon amounts in the soil may encourage a faster NO_3^- consumption.

Similarly, to the NO_3^- , N_2O was produced and consumed fast. It was consumed to levels below detection limit after timepoint T4, 14 days after resources were added, for all treatments (Fig. 6). The N_2O production was lowest and/or the N_2O consumption was highest in the control treatment, next lowest was *C2:N2*, followed by *C1:N2*. *C1:N1* had the highest production or lowest consumption among all treatments. The fact that *C2:N1* comes up as second to *C1:N1*, although the NO_3^- amounts are the same and the C: NO_3^- ratio actually is lower in *C2:N1* is interesting, although not significant. This implies, contrary to studies by Tiedje et al. (1983), Yoon et al. (2015), and Nojiri et al. (2020), that a higher amount of C resources and/or C: NO_3^- ratio could promote N_2O production or prevent N_2O consumption. The rate of consumption is important since it affects the net N_2O production, which is what would be emitted in the field. For further studying this, the genetic potential of N_2O consumption by reduction to nitrogen gas, quantification of the nitrous oxide reductase gene *nosZ* could be done. The production/consumption factors of net N_2O can be disentangled by using isotopic labelling of the NO_3^- , which would make it possible to track where the nitrogen ends up.

When comparing N_2O net production to the measured NO_3^- (Fig. 4), the two measurements reflect each other quite well, they are both consumed after just 14 days, but with N_2O dragging a bit after NO_3^- , as would be expected since NO_3^- must be reduced for N_2O to be produced.

NH_4^+ showed a somewhat reversed trend compared to NO_3^- and N_2O , increasing with time, the changes were, however, generally more gradual, except for between timepoint T5 and T6 and the concentrations are never at zero (Fig. 5). This underlines an important difference between nitrate and ammonium: ammonium is assimilated by most soil organisms for amino acid synthesis and is continuously released or mineralised, as they starve or die (Robertson & Groffman 2015). Although the NH_4^+ concentration was never zero, there was an initial decreasing trend with time for all treatments, but the control initially increased from T0 to T2, and for the high C low NO_3^- treatment *C1:N2* from T0 until T3. Then followed increases after 7 days, T3, gradual to timepoint T4 and T5 to across all treatments, with a somewhat more drastic increase from T4 to T5 for the *C1:N2*. Thereafter came quite a drastic increase from T5 to T6 for all treatments (Fig. 5). The first decrease of ammonium for all treatments but the control could be interpreted as immobilisation due to microbial growth (Robertson & Groffman 2015), the microorganisms are respiring with NO_3^- getting energy from organic C and assimilating C and NH_4^+ to build their cell biomass. The later increase matches with

the depletion of NO_3^- , as there would be less respiration and the microbes would start to starve or die.

The magnitude and range of this trend varied between the ratios, with $C1:N1$ and $C2:N1$ starting out as the lowest and ending with the highest NH_4^+ concentration (Fig. 5). The $C1:N2$, $C2:N2$ and the control treatments, having a low NO_3^- addition in common, started with higher concentrations and ended with lower concentrations compared to the other two ratios. The higher NH_4^+ concentrations at T1 may be explained by a lower microbial growth due to lower amounts of the electron acceptor. The final low concentrations may be caused by a lower microbial biomass exuding NH_4^+ .

This reasoning is also supported by the results from the quantification of the 16S rRNA marker gene assessing the quantity of bacteria and archaea. These results were almost an inverted mirroring of the NH_4^+ results (Fig. 7). Where the values of the NH_4^+ results were very similar for timepoints T1-T3 or showed a slight insignificant decrease timepoints T1-T3 are for 16S rRNA copies are also very similar to each other but with a slight insignificant increase in $C1:N1$. Interestingly, the low NO_3^- treatments, $C1:N2$ and $C2:N2$ also, as for NH_4^+ concentrations had a compact look when plotting, in other words that the growth and decrease is less notable than the high NO_3^- treatments, as well as for the control treatment. The first decrease from T0 to T1 that can be seen across all treatments, although not significant, suggests that it may be attributed to the soil condition rather than the treatment, perhaps an effect of the change to anoxic conditions induced 10 days and 12 days prior to sampling at T0 and T1. It is also notable that the low NO_3^- treatments at the beginning half of the experiment have similar values to the high NO_3^- treatments and ends with higher or similar values as the high NO_3^- treatments. Since these values are absolute and not relative, this makes it seem like the bacteria and archaea in treatments with less NO_3^- resources starved or died less or at least at similar rates to the treatments with more NO_3^- .

The genetic potential for denitrification (*nir* copies) were highest at timepoint T1 for the $C2:N1$ treatment with its low C: NO_3^- ratio of 4 (Fig. 8). This is in line with the hypothesis that low C: NO_3^- ratios promote denitrification (Tiedje et al. 1983; Yoon et al. 2015; Nojiri et al. 2020). There were, however, no significant differences between the treatments at this timepoint, or between any treatments at any timepoint (Table 11). At timepoint T0, *nir* copies were also interestingly high. There was then a decrease with every timepoint for all ratios but for $C1:N1$, where it instead increased at T1, T2 and T3 to then decrease for T4, increase again for T5 and finally drastically decrease at T6. A drastic decrease between timepoint T5 and T6 was apparent for all treatments (Fig 8).

The relative abundance of the *nir* marker gene showed the same pattern of quite a uniform decrease with time across all treatments (Fig. 9). All treatments started with similar values as T0 at T1, with a slight increase for *C1:N2* and *C2:N1*, and thereafter a gradual decrease until T6 where all treatments showed a dramatic decrease. There were no significant differences between the ratios at timepoint T1 and T2. The lower abundance at the first four days might suggest a competitive advantage for denitrifiers when the NO_3^- content still was relatively high for the treatments *C1:N1*, *C1:N2* and *C2:N1* (Fig. 4) and not yet a limitation. This does not, however, explain why the control and *C2:N2* was not significantly different from the treatments that still measured high NO_3^- after four days, maybe DNRA have a slow start from the freezer to start growing in the microcosms compared to denitrifiers.

After seven days, at timepoint T3, were the relative *nir* abundance of the high NO_3^- treatments significantly lower than that of the low NO_3^- treatments. The control was also significantly higher than all treatments but the low C, low NO_3^- treatment *C2:N2* (Table 12). At this timepoint, all NO_3^- was consumed except in *C1:N1*, intuitively the depletion of the electron acceptor would be expected to cause a decrease of relative *nir* abundance in all treatments but *C1:N1*, but the opposite was seen (Fig. 9). This seemingly delayed response to lowered NO_3^- , however odd, could be explained by denitrifiers going into a dormant state, respiring less while still showing the same number of *nir* gene copies. This was somewhat reflected in the 16S rRNA results that showed very similar values for T1-T3, except for *C1:N1*. The production and consumption of N_2O within the same timeframe that NO_3^- was consumed suggest that these nitrogen measurements might reflect the actual denitrification better than the genetic potential for the individual *nir* and *nrfA* measurements does.

Quantification of the *nrfA* marker gene through qPCR showed less of a pattern than the other genes and soil nitrogen and gas measurements (Fig. 10). The statistical analysis showed that no group was significantly different to any other group, neither were any treatment different from any other treatment when compared at each timepoint (Table 13). However, the relative *nrfA* abundance showed a opposite trend compared to that of the *nir*, as the *nir* portion of the bacterial and archaeal abundance did decrease with time the *nrfA* portion increased. The same ambiguousness that *nir* showed around the timepoints T1-T3 that were so important in net N_2O production and NO_3^- consumption. The general pattern of an increase towards the end of the experiment implies that at least some parts of the DNRA group are more resistant than the denitrifiers. This could be because they have a much higher affinity to NO_3^- , are able to gain energy from an alternative pathway,

and/or enter a dormant state which they manage better than denitrifiers. This could be a highly interesting characteristic when studying functional microbial community changes over many pulses of added resources followed by starvation. This could potentially further imply that recreating such conditions with repeated NO_3^- starvation could promote a microbial community more prone to DNRA.

Furthermore, it is surprising to find that the *nrfA* abundance is greater than the *nir* abundance since the opposite has been assumed for agricultural soils and also demonstrated in the microcosm experiment by Putz et al (2018). The soil used was from a low fertilisation treatment of a long-term field experiment, but normally this would not be expected of agricultural soils with high nitrogen concentrations and low C: NO_3^- ratios. This can be observed more clearly from the *nrfA/nir* (Fig. 12). The *nrfA* abundance was always higher than the *nir*, for all groups. The increasing trend over time also highlights DNRA's supposed resistance compared to denitrifiers. The clearest difference between treatments was between the *C1:N1* treatment and the other treatments, the first five timepoints showed comparatively low values, similar to T1 of most treatments, and little change. This means, for the experiment, a higher genetic potential for denitrification compared to DNRA for timepoint T1-T5. This is notable as there is a more gradual increase for all other treatments.

4.2 Correlations between changes in N pools and/or net N_2O production and the abundance of functional communities

The second aim of this experiment was to test for correlations between the nitrogen measurements and the abundance of functional communities for discussing functionality of the microbiome in the studied soil.

Using Spearman's rank test to test for correlations between the measurements, showed a significant strong positive correlation between net N_2O production and *nir* abundance (Fig. 15). This was expected since denitrification produce N_2O and only 40% of denitrifiers are estimated to possess the *nos* gene encoding the nitrous oxide reductase enzyme (Graf et al. 2014). Although the N_2O also was fully consumed at some point it was detected in the gas headspace of the microcosms, meaning that it had left the cell and would have been emitted to the atmosphere if not for the closed environment. The consumption was probably mostly due to depletion of any other electron acceptor, when microbes possessing the genetic potential for N_2O respiration could use that to still gain energy.

In contrary, the significant moderate positive correlation between N₂O net production and *nrfA* was more surprising, N₂O has been shown to be produced by DNRA but in comparatively negligible amount. This could be indicating that N₂O production by DNRA could be more important in agricultural soils, or in this particular soil (Rütting et al. 2011; Stremińska et al. 2012). If that were to be confirmed by further studies, it would be very relevant for our understanding of soil microbial communities in general and to how we can manage our soils to mitigate greenhouse gas emissions. It was however incidental since correlation between N₂O net production and the *nrfA/nir* ratio was tested it showed to be significantly moderately negative, which is what was expected. As the *nrfA/nir* ratio in this experiment always was above one, *nrfA* was always higher than *nir*, an increasing ratio means increasing how much higher *nrfA* was compared to *nir*. The bigger the portion of NO₃⁻ respiring organisms that were DNRA the less N₂O was produced.

For the soil nitrogen pools, NO₃⁻ showed a strong significant positive correlation with N₂O net production, as previously found (Lebender et al. 2014). NO₃⁻ fertilisation was linked to N₂O production also in this soil (Fig. 13). The significant strong negative correlation of NH₄⁺, 16S rRNA and *nir* (Fig. 18) was also expected because, as discussed, a growing microbial community will assimilate NH₄⁺ and a starving and or dying community will release NH₄⁺. However, the case is different for *nrfA* since NH₄⁺ is also produced through NO₃⁻ respiration. This could explain why the moderate negative correlation (Fig. 14) is surprising but can be explained as an effect of mineralisation for the whole community being bigger than production by DNRA, and by the supposed resistance of DNRA through starvation. When the NH₄⁺ was tested against the relative abundance of *nrfA* there was a moderate positive correlation while it showed no correlation with the relative abundance of *nir*. This theoretically makes more sense: a whole starving community is related to increasing NH₄⁺ levels, the *nrfA*-carrying members of that community compared to the whole is positively correlated since they produce NH₄⁺ and the *nir* part of that community compared to the whole is not correlated since that functional group is no different from the whole for that aspect.

4.3 Take-aways from this pilot study and method discussion

The third aim of this experiment was that the results would inform a bigger experiment on methodology and tendencies of this particular soil.

Soil from Lönnstorp of the treatment with 40 kg/ha nitrogen fertilisation and incorporated straw showed a rapid consumption of NO₃⁻ and N₂O. This implies that

the microbes in all treatments experienced starvation within 7-14 days, although decreases of marker genes imply that they were still present in the soil without respiring for some time before they decreased.

If changes in microbial functional composition were to be studied over longer time and over many pulses of added resources, it would be beneficial to include more timepoints between the addition and 14 days after. If the goal is just to subject the NO_3^- respiring organisms to starvation then 14 days are enough, and the timeframe of the experiment could be shortened. However, if the goal is to have the organisms experience lethal effects of starvation 40 days of incubation, comparative to T6, might be needed between pulses.

The efficiency of studying functional genes can also be questioned as they, as shown in in this experiment and other studies (Rocca et al. 2015), do not always accurately match the rates of denitrification and DNRA but solely the genetic potential. As mentioned previously, the inclusion of *nosZ* as a marker gene would also be interesting for a bigger experiment. Although it seemingly does not help the study of controls of the partitioning of nitrate between DNRA and denitrifiers, it would aid for one of the larger applied goals of such a study: how do we mitigate N_2O emissions from agriculture practises. Also, in conclusion of previous arguments, ^{15}N isotopic labelling of the added NO_3^- would clarify the relationships between the nitrogen measurements that are still a bit cryptic in this study.

The continually high *nrfA* copy numbers, in addition to the low efficiency of the qPCR runs (Table 5), might suggest there is room for development of either primers or protocols. This experiment also used primers and protocol by Cannon et al. (2019) while for example Putz et al. (2018) used primers and protocol by Welsh et al. (2014). Low efficiency may also inaccurate standard curves or pipetting, this risk is minimized by having two independent runs show comparable results (Thermo Fisher n.d.). It may also be a consequence of PCR-inhibitory contaminants in the DNA extraction, which the inhibition test showed but very slight and sample volumes were lowered from 4 to 3 uL to prevent any inhibition in the runs. The runs for the other genes were also less affected, had higher efficiency. The efficiencies where problematic across the board, which is why some assessments of the equipment also should be considered before conducting a bigger experiment based on the same methodology as described in this study.

Other methodologically important finding from this experiment is that there were unexpectedly high NH_4^+ concentrations in the KCl blanks. After some tests we concluded that it may come from the dish soap that is used to clean the excipient, or from the plastic 50 mL Facon tubes used. Although this was correctable by subtracting the blank values it shows that it would be highly useful to set up

equipment for acid washing glassware and develop a protocol for doing the extractions in reusable glass containers.

Further, for the N₂O measurements analysed by gas chromatography, the high concentration in the beginning timepoint of the experiment, T1-T3, complicated the procedure to make all samples comparable. The procedure of taking extra samples from timepoints within that timeframe is advisable for a bigger experiment. For data analysis, the tests used in the present study, Kruskal-Wallis, post hoc Fisher's least significant difference and Spearman's correlation test, could probably also be used for a bigger experiment. It would then be advisable to use more replicates to get more accurate results.

5. Conclusions

Microorganisms with genetic potential to perform DNRA were surprisingly overall more abundant than the denitrifying community. Further, the *nrfA/nir* ratio increased over time, indicating that DNRA could be more resistant to starvation compared to denitrifiers, which is of interest for long-term microcosm experiments. The NO_3^- , N_2O , NH_4^+ and 16S rRNA measurements support previous findings and theory that NO_3^- is consumed as N_2O is being produced, that there is some denitrifiers that are unable to perform complete denitrification which results in net N_2O production, and that ammonium is immobilized and mineralised as the microbial community increase and decrease.

There were differences between treatments, they were most clear for the NO_3^- and N_2O measurements, they do however not definitely support that low C: NO_3^- promotes denitrifiers, as measured by net N_2O production. High added NO_3^- amounts does however seem to have a positive effect but that effect, further, seems only to enhance denitrification. This reasoning is however not completely valid without differentiating the production and consumption factors that contribute to the net N_2O production. For this reason, inclusion of the *nosZ* marker gene would be interesting for further studies, especially as an experiment over longer time might show more response in the marker genes.

Differences between the treatments for denitrification vs. DNRA was quite unclear. The most notable is that a treatment with high C, high NO_3^- and a C: NO_3^- ratio of 40 that had the highest genetic potential for denitrification compared to DNRA. This paired with the N_2O net production, and comparatively low relative *nrfA* abundance for the same treatment point to that High NO_3^- and high C promotes denitrification over DNRA. This finding is contradicting many other studies and is probably mostly due to the continually high genetic potential for DNRA which makes it hard to draw any conclusions on what treatments that promotes DNRA. Significance was an overall problem in this study especially with the marker genes, although the observed trends could have some interesting implications. Without consistent significant differences between the groups for all the three measurements of denitrifier and DNRA activity it is hard to confidently draw conclusions on the effect of different treatments at different timepoints. That said, the soil microbiome is inherently very complex and its dynamics might not be easily explained. Most importantly, the unusually high abundance of DNRA in the soil used in this experiment makes it highly interesting for further studies to investigate if it is an effect of short-term treatments, of a long-term soil management history or physical soil characteristics.

References

- Brody, J.R. & Kern, S.E. (2004). Sodium boric acid: a Tris-free, cooler conductive medium for DNA electrophoresis. *BioTechniques*, 36 (2), 214–216. <https://doi.org/10.2144/04362BM02>
- Cannon, J., Sanford, R.A., Connor, L., Yang, W.H. & Chee-Sanford, J. (2019). Optimization of PCR primers to detect phylogenetically diverse *nrfA* genes associated with nitrite ammonification. *Journal of Microbiological Methods*, 160, 49–59. <https://doi.org/10.1016/j.mimet.2019.03.020>
- Carlson, H.K., Lui, L.M., Price, M.N., Kazakov, A.E., Carr, A.V., Kuehl, J.V., Owens, T.K., Nielsen, T., Arkin, A.P. & Deutschbauer, A.M. (2020). Selective carbon sources influence the end products of microbial nitrate respiration. *The ISME Journal*, 14 (8), 2034–2045. <https://doi.org/10.1038/s41396-020-0666-7>
- Dari, B., Rogers, C.W. & Walsh, O.S. (u.å.). Understanding Factors Controlling Ammonia Volatilization from Fertilizer Nitrogen Applications. 4
- DNASU (2022) *Plasmid | Detailed Vector Information: pCR4*. *DNASU Plasmids*. <http://dnasu.org/DNASU/GetVectorDetail.do?vectorid=287> [2022-08-11]
- Frette, L., Gejlsbjerg, B. & Westermann, P. (1997). Aerobic denitrifiers isolated from an alternating activated sludge system. *FEMS Microbiology Ecology*, 24 (4), 363–370. <https://doi.org/10.1111/j.1574-6941.1997.tb00453.x>
- Graf, D.R.H., Jones, C.M. & Hallin, S. (2014). Intergenomic Comparisons Highlight Modularity of the Denitrification Pathway and Underpin the Importance of Community Structure for N₂O Emissions. *PLOS ONE*, 9 (12), e114118. <https://doi.org/10.1371/journal.pone.0114118>
- Hachiya, T. & Sakakibara, H. (2017). Interactions between nitrate and ammonium in their uptake, allocation, assimilation, and signaling in plants. *Journal of Experimental Botany*, 68 (10), 2501–2512. <https://doi.org/10.1093/jxb/erw449>
- Hallin, S., Philippot, L., Löffler, F.E., Sanford, R.A. & Jones, C.M. (2018). Genomics and Ecology of Novel N₂O-Reducing Microorganisms. *Trends in Microbiology*, 26 (1), 43–55. <https://doi.org/10.1016/j.tim.2017.07.003>
- Hayatsu, M., Tago, K. & Saito, M. (2008). Various players in the nitrogen cycle: Diversity and functions of the microorganisms involved in nitrification and denitrification. *Soil Science & Plant Nutrition*, 54 (1), 33–45. <https://doi.org/10.1111/j.1747-0765.2007.00195.x>
- Heo, H., Kwon, M., Song, B. & Yoon, S. (2020). Involvement of NO₃⁻ in Ecophysiological Regulation of Dissimilatory Nitrate/Nitrite Reduction to Ammonium (DNRA) Is Implied by Physiological Characterization of Soil DNRA Bacteria Isolated via a Colorimetric Screening Method. *Applied and Environmental Microbiology*, 86 (17), e01054-20. <https://doi.org/10.1128/AEM.01054-20>
- Körner, H., Sofia, H.J. & Zumft, W.G. (2003). Phylogeny of the bacterial superfamily of Crp-Fnr transcription regulators: exploiting the metabolic

- spectrum by controlling alternative gene programs. *FEMS microbiology reviews*, 27 (5), 559–592. [https://doi.org/10.1016/S0168-6445\(03\)00066-4](https://doi.org/10.1016/S0168-6445(03)00066-4)
- Lebender, U., Senbayram, M., Lammel, J. & Kuhlmann, H. (2014). Impact of mineral N fertilizer application rates on N₂O emissions from arable soils under winter wheat. *Nutrient Cycling in Agroecosystems*, 100 (1), 111–120. <https://doi.org/10.1007/s10705-014-9630-0>
- Moir, J. & Wood, N. (2001). Nitrate and nitrite transport in bacteria. *Cellular and molecular life sciences : CMLS*, 58, 215–24. <https://doi.org/10.1007/PL00000849>
- Nojiri, Y., Kaneko, Y., Azegami, Y., Shiratori, Y., Ohte, N., Senoo, K., Otsuka, S. & Isobe, K. (2020). Dissimilatory Nitrate Reduction to Ammonium and Responsible Microbes in Japanese Rice Paddy Soil. *Microbes and Environments*, 35 (4), ME20069. <https://doi.org/10.1264/jsme2.ME20069>
- Oelmann, Y., Kreutziger, Y., Bol, R. & Wilcke, W. (2007). Nitrate leaching in soil: Tracing the NO₃⁻ sources with the help of stable N and O isotopes. *Soil Biology and Biochemistry*, 39 (12), 3024–3033. <https://doi.org/10.1016/j.soilbio.2007.05.036>
- Parada, A.E., Needham, D.M. & Fuhrman, J.A. (2016). Every base matters: assessing small subunit rRNA primers for marine microbiomes with mock communities, time series and global field samples. *Environmental Microbiology*, 18 (5), 1403–1414. <https://doi.org/10.1111/1462-2920.13023>
- Poor PCR Efficiency - SE (u.å.). <https://www.thermofisher.com/uk/en/home/life-science/pcr/real-time-pcr/real-time-pcr-learning-center/real-time-pcr-basics/real-time-pcr-troubleshooting-tool/gene-expression-quantitation-troubleshooting/poor-pcr-efficiency.html> [2022-06-18]
- Putz, M., Schleusner, P., Rütting, T. & Hallin, S. (2018). Relative abundance of denitrifying and DNRA bacteria and their activity determine nitrogen retention or loss in agricultural soil. *Soil biology & biochemistry*, 123, 97–104. <https://doi.org/10.1016/j.soilbio.2018.05.006>
- Robertson, G.P. & Groffman, P.M. (2015). Chapter 14 - Nitrogen Transformations. I: Paul, E.A. (red.) *Soil Microbiology, Ecology and Biochemistry (Fourth Edition)*. Boston: Academic Press, 421–446. <https://doi.org/10.1016/B978-0-12-415955-6.00014-1>
- Rocca, J.D., Hall, E.K., Lennon, J.T., Evans, S.E., Waldrop, M.P., Cotner, J.B., Nemergut, D.R., Graham, E.B. & Wallenstein, M.D. (2015). Relationships between protein-encoding gene abundance and corresponding process are commonly assumed yet rarely observed. *The ISME Journal*, 9 (8), 1693–1699. <https://doi.org/10.1038/ismej.2014.252>
- Rütting, T., Boeckx, P., Müller, C. & Klemmedtsson, L. (2011). Assessment of the importance of dissimilatory nitrate reduction to ammonium for the terrestrial nitrogen cycle. *Biogeosciences*, 8 (7), 1779–1791. <https://doi.org/10.5194/bg-8-1779-2011>
- Schlesinger, W. & Bernhardt, E. (2013). The Global Cycles of Nitrogen and Phosphorus. 445–467. <https://doi.org/10.1016/B978-0-12-385874-0.00012-1>
- Spiro, S. (2007). Regulators of bacterial responses to nitric oxide. *FEMS Microbiology Reviews*, 31 (2), 193–211. <https://doi.org/10.1111/j.1574-6976.2006.00061.x>
- Steffen, W., Richardson, K., Rockström, J., Cornell, S.E., Fetzer, I., Bennett, E.M., Biggs, R., Carpenter, S.R., de Vries, W., de Wit, C.A., Folke, C., Gerten, D., Heinke, J., Mace, G.M., Persson, L.M., Ramanathan, V., Reyers, B. & Sörlin, S. (2015). Planetary boundaries: Guiding human development on a changing planet. *Science*, 347 (6223), 1259855. <https://doi.org/10.1126/science.1259855>

- Stremińska, M.A., Felgate, H., Rowley, G., Richardson, D.J. & Baggs, E.M. (2012). Nitrous oxide production in soil isolates of nitrate-ammonifying bacteria. *Environmental Microbiology Reports*, 4 (1), 66–71. <https://doi.org/10.1111/j.1758-2229.2011.00302.x>
- Strohm, T.O., Griffin, B., Zumft, W.G. & Schink, B. (2007). Growth yields in bacterial denitrification and nitrate ammonification. *Applied and Environmental Microbiology*, 73 (5), 1420–1424. <https://doi.org/10.1128/AEM.02508-06>
- Throbäck, I.N., Enwall, K., Jarvis, A. & Hallin, S. (2004). Reassessing PCR primers targeting nirS, nirK and nosZ genes for community surveys of denitrifying bacteria with DGGE. *FEMS microbiology ecology*, 49 (3), 401–417. <https://doi.org/10.1016/j.femsec.2004.04.011>
- Tiedje, J.M., Sexstone, A.J., Myrold, D.D. & Robinson, J.A. (1983). Denitrification: ecological niches, competition and survival. *Antonie van Leeuwenhoek*, 48 (6), 569–583. <https://doi.org/10.1007/BF00399542>
- Trevors, J.T. (1985). The influence of oxygen concentrations on denitrification in soil. *Applied Microbiology and Biotechnology*, 23 (2), 152–155. <https://doi.org/10.1007/BF00938969>
- Vuono, D.C., Read, R.W., Hemp, J., Sullivan, B.W., Arnone, J.A., Neveux, I., Blank, R.R., Loney, E., Miceli, D., Winkler, M.-K.H., Chakraborty, R., Stahl, D.A. & Grzymiski, J.J. (2019). Resource Concentration Modulates the Fate of Dissimilated Nitrogen in a Dual-Pathway Actinobacterium. *Frontiers in Microbiology*, 10. <https://www.frontiersin.org/article/10.3389/fmicb.2019.00003> [2022-02-02]
- Welsh, A., Chee-Sanford, J.C., Connor, L.M., Löffler, F.E. & Sanford, R.A. (2014). Refined NrfA phylogeny improves PCR-based nrfA gene detection. *Applied and Environmental Microbiology*, 80 (7), 2110–2119. <https://doi.org/10.1128/AEM.03443-13>
- Yoon, S., Cruz-García, C., Sanford, R., Ritalahti, K.M. & Löffler, F.E. (2015). Denitrification versus respiratory ammonification: environmental controls of two competing dissimilatory NO₃⁻/NO₂⁻ reduction pathways in *Shewanella loihica* strain PV-4. *The ISME Journal*, 9 (5), 1093–1104. <https://doi.org/10.1038/ismej.2014.201>

Popular science summary

Nitrogen is an important resource as a plant nutrient, we need to increase plant production to have food for all. There are, however, problems with nitrogen fertilisation, that often come in three different forms: organic e.g. manure, ammonium, and nitrate. Ammonium can also be transformed to nitrate by microorganisms in the soil. Nitrate makes plants grow better but it can also leach out of the soil into nearby waters where the excess nutrients can cause eutrophication. Secondly, nitrate can be used by some microorganisms to respire when there is no oxygen in the soil, for example when it is very wet. There are two groups that can do this, denitrifying microorganisms called denitrifiers and microorganisms that perform dissimilatory nitrogen reduction to ammonium, DNRA for short. Denitrifiers transform the nitrate into two other forms of nitrogen, nitrogen gas that is the most common gas in the atmosphere and nitrous oxide that is a potent greenhouse gas 300 times stronger than carbon dioxide. DNRA, on the other hand, transforms the nitrate into ammonium that can be taken up by plants. Since the two groups both use nitrate to respire, they are competing for it in the soil, and if we can find out what factors promote DNRA and/or disfavour denitrifiers we could decrease the greenhouse gas emissions produced by agriculture and keep nitrogen in the soil in a form that plants can use.

This experiment aimed to test three factors that other experiments have found is important to make DNRA grow better than denitrifiers, namely how much carbon there is in the soil, how much nitrate there is in the soil and the ratio between the carbon and the nitrate amounts. Researchers have found that less nitrate compared to carbon makes DNRA grow better than denitrifiers when they were grown in a laboratory. It is suggested that DNRA is better at getting energy from carbon and therefore use less nitrate for respiration compared to denitrification.

The most important conclusions from this experiment are: 1) The results from the soil we used were a bit different from previous experiments, there were always more DNRA than denitrifiers, which makes the soil we used very interesting. 2) It was hard to tell how carbon and nitrate affected the competition between DNRA and denitrifiers.

Acknowledgements

I would like to give special thanks to my supervisor Aurélien Saghai for all help and his efforts to make me feel included in the research and community at the department.

I would also like to thank the Department of Forest Mycology and Plant Pathology and the soil microbiology group, especially Christopher Jones and Jaanis Juhanson for their help with difficult machines and troubleshooting.

Appendix 1



A044 R3 Nitrate
Nitrite MT519.pdf



A048 R1 Ammonia
(soil) MT507.pdf

Publishing and archiving

Approved students' theses at SLU are published electronically. As a student, you have the copyright to your own work and need to approve the electronic publishing. If you check the box for **YES**, the full text (pdf file) and metadata will be visible and searchable online. If you check the box for **NO**, only the metadata and the abstract will be visible and searchable online. Nevertheless, when the document is uploaded it will still be archived as a digital file. If you are more than one author, the checked box will be applied to all authors. Read about SLU's publishing agreement here:

- <https://www.slu.se/en/subweb/library/publish-and-analyse/register-and-publish/agreement-for-publishing/>.

YES, I/we hereby give permission to publish the present thesis in accordance with the SLU agreement regarding the transfer of the right to publish a work.

NO, I/we do not give permission to publish the present work. The work will still be archived and its metadata and abstract will be visible and searchable.